Surface Water and Ocean Topography (SWOT) Project
SWOT Product Description
Long Name: Level 2 KaRIn high rate water mask pixel cloud product
Short Name: L2_HR_PIXC

Revision C

Document Custodians:

Electronic Signature on File
17-Mar-2025

Brent Williams
JPL Algorithm Engineer

E-SIGNED by Roger Fjortoft
on 2025-03-31 06:43:26 GMT

Roger Fjørtoft
CNES Algorithm Engineer

Approved by:

Electronic Signature on File
17-Mar-2025

Curtis Chen
JPL Algorithm System Engineer

E-SIGNED by Roger Fjortoft
on 2025-03-31 06:43:30 GMT

Roger Fjørtoft
CNES Algorithm System Engineer

Concurred by:

Electronic Signature on File
24-Mar-2025

Stirling Algermissen
JPL SDS Manager

E-SIGNED by Pierre-Marie Brunet
on 2025-04-02 06:44:41 GMT

Lionel Zawadzki
CNES Hydrology Distribution Center Manager

Paper copies of this document may not be current and should not be relied on for official purposes. The current version is in the JPL Engineering Product Data Management system (EPDM: https://epdm.jpl.nasa.gov) and the CNES Product Data Management System

See Sect 1.4 for how to cite this document

February 24, 2025
JPL D-56411

National Aeronautics and Space Administration
Jet Propulsion Laboratory
California Institute of Technology

© 2025 California Institute of Technology. Government sponsorship acknowledged.

EPDM ELECTRONIC SIGNATURES

Status	Performer	Assignee Ori…	Due Date	End Date
Approve	Algermissen, Stirling S (alge…	Document Appro…	25-Mar-2025 10:00	24-Mar-2025
Approve	Williams, Brent A (bawillia)	Document Appro…	25-Mar-2025 10:00	17-Mar-2025
Approve	Chen, Curtis W (curtis)	Document Appro…	25-Mar-2025 10:00	17-Mar-2025

CHANGE LOG

VERSION	DATE	SECTIONS CHANGED	REASON FOR CHANGE
Preliminary	2017-02-16	ALL	Preliminary version Approved for export (LRR-028890)
Initial Release	2019-02-11	ALL	Initial release Approved for public release (URS280883/CL#19-0855)
Revision A (DRAFT)	2020-08-10	ALL	Revision A (draft for sample data) Approved for public release (URS294013/CL#20-3591)
Revision A	2022-09-20	ALL	Revision A Approved for public release (URS311045/CL#22-4904)
Revision B	2023-10-26	4.1.2.1, 5.2	Revision B Sect 4.1.2.1: Clarify interferogram_size_azimuth. Sect 5.2: Split some xref global attributes, added bit for pixc_line_qual and added quality bits for in air pixels and specular ringing. Added variables indicating data window first and last valid pixel and first and lass cross-track for each azimuth line. Approved for public release (URS320829/CL#23-6134)
Revision C (DRAFT)	2024-10-23	5.2.3	Add variable prior_water_change. Add suspect_karin_telem bit flag to interferogram_qual, classification_qual, geolocation_qual, sig0_qual, pixc_line_qual. Adopt FES2022b load tide model.
Revision C	2025-02-24	See above	Revision C Approved for public release (URS331720/CL#25-1009)

© 2025 California Institute of Technology. Government sponsorship acknowledged.

Table of Contents

CHANGE LOG **2**

Table of Contents **3**

Table of Figures **5**

Table of Tables **6**

List of TBC Items **7**

List of TBD Items **7**

1 Introduction **8**
1.1 Purpose **8**
1.2 Document Organization **8**
1.3 Document Conventions **8**
1.4 Citing This Document **8**

2 Product Description **9**
2.1 Purpose **9**
2.2 Latency **12**

3 Product Structure **13**
3.1 Granule Definition **13**
3.2 File Organization **14**
3.3 File Naming Convention **15**
3.4 Spatial Sampling and Resolution **16**
3.5 Temporal Organization **19**
3.6 Spatial Organization **19**
3.7 Volume **21**

4 Qualitative Description **23**
4.1 Level 2 KaRIn HR Pixel Cloud Data File **23**
4.1.1 Global Attributes 24
4.1.2 Pixel Cloud Group Data 25
4.1.2.1 Pixel Cloud Group Attributes 25
4.1.2.2 Rare Layer 26
4.1.2.3 Medium Layer 28
4.1.3 TVP Group Data 34
4.1.3.1 Time 35
4.1.3.2 Location, Velocity and Attitude 35
4.1.3.3 Antenna Phase Center Positions 36
4.1.3.4 Index in HR Data Collection 36
4.1.3.5 Flags 36
4.1.4 Noise Group Data 38

5 Detailed Product Description **39**
5.1 NetCDF Variables **39**
5.2 Level 2 KaRIn HR Pixel Cloud File **40**

6 References **61**

Appendix A. **Acronyms** **62**

© 2025 California Institute of Technology. Government sponsorship acknowledged.

Appendix B. **Quality Flag Bit Definitions 64**

© 2025 California Institute of Technology. Government sponsorship acknowledged.

Table of Figures

FIGURE 1. SIMULATED EXAMPLE OF THE LATITUDE (A), LONGITUDE (B), HEIGHT (C), AND RADAR ECHO POWER (D) FROM THE L2_HR_PIXC PRODUCT, REPRESENTED AS SPARSE 2-D SLANT-PLANE ARRAYS.....11
FIGURE 2. SIMULATED EXAMPLE OF THE HEIGHT FROM THE L2_HR_PIXC PRODUCT PROJECTED INTO THE GROUND PLANE (LEFT) AND REPRESENTED AS A 3-D POINT CLOUD (RIGHT). 11
FIGURE 3. L2_HR_PIXC PRODUCT GRANULE ILLUSTRATION.....14
FIGURE 4. SLC IMAGE DIMENSIONS. 16
FIGURE 5. NOTIONAL ILLUSTRATION OF THE RELATIONSHIPS BETWEEN THE POSTING AND INFORMATION CONTENT OF SLC ("RAW"), RARE, AND MEDIUM SAMPLES IN THE SLANT PLANE. 17
FIGURE 6. CONCEPTUAL ILLUSTRATION OF THE RELATIONSHIPS BETWEEN THE SAMPLING OF THE *TVP*, *NOISE*, AND *PIXEL_CLOUD* GROUPS WITH RESPECT TO THE SLC SAMPLING GRID. 20
FIGURE 7. ILLUSTRATION OF THE KMSF FRAME AND THE POLARIZATIONS (V AND H) OF THE TWO KARIN HALF SWATHS. THE VELOCITY DIRECTION CAN BE ALONG $+X_{KMSF}$ OR $-X_{KMSF}$ DEPENDING ON THE YAW STATE OF THE SPACECRAFT.....23

© 2025 California Institute of Technology. Government sponsorship acknowledged.

Table of Tables

TABLE 1. DESCRIPTION OF THE FILE COMPRISING THE L2_HR_PIXC PRODUCT. 14
TABLE 2: DESCRIPTION OF THE NETCDF GROUPS IN L2_HR_PIXC PRODUCT. 15
TABLE 3: DESCRIPTION OF THE DATA VOLUME OF THE L2_HR_PIXC PRODUCT. 22
TABLE 4. VARIABLE DATA TYPES IN NETCDF PRODUCTS. 39
TABLE 5. COMMON VARIABLE ATTRIBUTES IN NETCDF FILES. 39
TABLE 6. GLOBAL ATTRIBUTES FOR ALL DATA GROUPS IN THE L2_HR_PIXC PRODUCT FILE. 40
TABLE 7. ATTRIBUTES OF THE *PIXEL_CLOUD* GROUP OF THE L2_HR_PIXC PRODUCT. 43
TABLE 8. ATTRIBUTES OF THE *TVP* GROUP OF THE L2_HR_PIXC PRODUCT. 43
TABLE 9. ATTRIBUTES OF THE *NOISE* GROUP OF THE L2_HR_PIXC PRODUCT. 43
TABLE 10. DIMENSIONS OF VARIABLES WITHIN EACH NETCDF DATA GROUP. 43
TABLE 11. VARIABLES OF THE *PIXEL_CLOUD* GROUP OF THE L2_HR_PIXC PRODUCT. 44
TABLE 12. VARIABLES OF THE TVP GROUP OF THE L2_HR_PIXC PRODUCT. 56
TABLE 13. VARIABLES OF THE NOISE GROUP OF THE L2_HR_PIXC PRODUCT 60
TABLE 14. BIT FLAG EXAMPLE 64
TABLE 15. MEASUREMENT QUALITY FLAG BIT DEFINITIONS 64

© 2025 California Institute of Technology. Government sponsorship acknowledged.

List of TBC Items

Page	Section

List of TBD Items

Page	Section

© 2025 California Institute of Technology. Government sponsorship acknowledged.

1 Introduction

1.1 Purpose

The purpose of this Product Description Document is to describe the Level 2 Ka-band Radar Interferometer (KaRIn) high rate (HR) water mask pixel cloud data product from the Surface Water Ocean Topography (SWOT) mission. This data product is also referenced by the short name L2_HR_PIXC.

1.2 Document Organization

Section 2 provides a general description of the product, including its purpose and latency.

Section 3 provides the structure of the product, including granule definition, file organization, spatial resolution, temporal and spatial organization of the content, the size and data volume.

Section 4 provides qualitative descriptions of the information provided in the product.

Section 5 provides a detailed identification of the individual fields within the L2_HR_PIXC product, including for example their units, size, coordinates, etc.

1.3 Document Conventions

When the specific names of data variables and groups of the data product are given in the body text of this document, they are usually represented in italicized text.

1.4 Citing This Document

Please cite this document as follows:

> JPL D-56411, Revision C, “SWOT Product Description Document: Level 2 KaRIn High Rate Water Mask Pixel Cloud (L2_HR_PIXC) Data Product,” Jet Propulsion Laboratory Internal Document, 2025.

© 2025 California Institute of Technology. Government sponsorship acknowledged.

2 Product Description

2.1 Purpose

The L2_HR_PIXC product contains measured height, geolocation, and classification data from the high-rate (HR) data stream of the KaRIn instrument. These data are generally produced for inland and coastal hydrology surfaces, as controlled by the reloadable KaRIn HR mask. The L2_HR_PIXC product is produced using algorithms that are detailed in [1]. Note that the SWOT low-rate (LR) data stream and its associated data products may be more appropriate for large water features since the LR data allow for finer vertical precision, albeit at coarser horizontal resolution; the geophysical corrections included in the LR data products also differ from those of the L2_HR_PIXC product. The L2_HR_PIXC product is generated in response to the SWOT project science requirements described in [2].

While KaRIn HR data are collected over two continuous half-swaths on either side of the nadir track, the great majority of samples over land are too noisy to be useful given the low radar reflectivity of land (as compared to water). Consequently, only a small subset of the downlinked data, corresponding primarily to water, are stored in the pixel cloud data product.

For each sample in the pixel cloud, the product contains the following:

1. Geolocated elevations (latitude, longitude, and height)
2. Classification mask (water/land flags, and water fraction)
3. Surface areas (projected pixel area on the ground)
4. Relevant data needed to compute and aggregate height and area uncertainties

Additional information is also provided to improve the utility of the product and to facilitate generation of downstream products. This information includes:

1. Meta data (global instrument parameters)
2. Time varying parameters (TVP), which include sensor position, velocity, attitude, and time
3. Noise power estimates
4. Quality flags
5. Interferogram measurements (power and phase) and range and azimuth indices
6. Geophysical and crossover-calibration correction values

Note that river and lake vector processing provide a few additional fields that complement the data in the L2_HR_PIXC product. The additional data from river and lake vector processing are generated on the same posting and over the same granules as data in the L2_HR_PIXC product. This complementary information (e.g., smoothed geolocations, and pixel assignment mappings to the river and lake features) is available in an add-on companion product to the L2_HR_PIXC product called the L2_HR_PIXCVec product (see [3] for more information on the L2_HR_PIXCVec product).

As an illustrative example, Figure 1 shows some of the information in the L2_HR_PIXC product from a simulation. Each panel shows one quantity from the product represented as a sparsely populated 2-D array in the native range-azimuth or ‘slant-plane’ sampling coordinates of the radar (see Section 3.4 for more detail). Many other quantities are included in the product

© 2025 California Institute of Technology. Government sponsorship acknowledged.

but are not shown here. Together, the *latitude* (a), *longitude* (b), and *height* (c) variables give the observed location of each sample in 3-D space. Other quantities such as the radar echo power (d) and the classification (not shown, but closely related to the echo power) are also given for each sample in the product.

The left panel of Figure 2 shows the 3-D locations of the samples in Figure 1 as heights projected into the ground plane (i.e., as functions of latitude and longitude). The nature of the SWOT measurement is such that measurement noise gives cross-track horizontal errors (primarily longitude variability in this example) in addition to height errors. The right panel of Figure 2 shows the 3-D locations of a portion of the data set as a cloud of points in 3-D space, along with error bars for each point. The darker land pixels surrounding the water pixels of the river have lower signal-to-noise ratio (SNR) and hence larger height uncertainties.

Note that while the data of Figure 1 and Figure 2 are shown as sparsely populated 2-D arrays, the data are stored in the product as 1-D arrays along with the information to reconstruct the sparse 2-D arrays (see Sections 3.6 and 4.1.2.2).

© 2025 California Institute of Technology. Government sponsorship acknowledged.

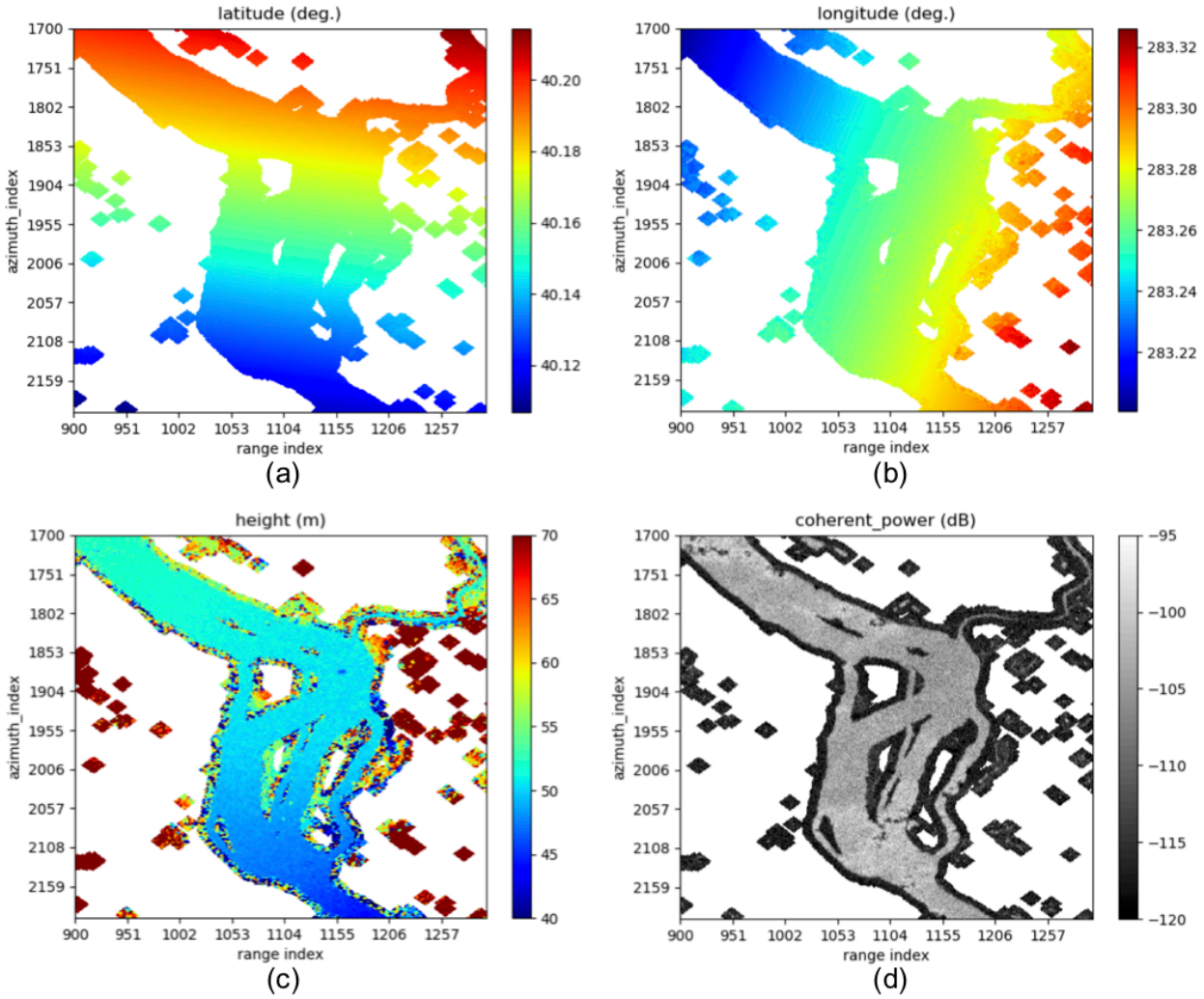

Figure 1. Simulated example of the latitude (a), longitude (b), height (c), and radar echo power (d) from the L2_HR_PIXC product, represented as sparse 2-D slant-plane arrays.

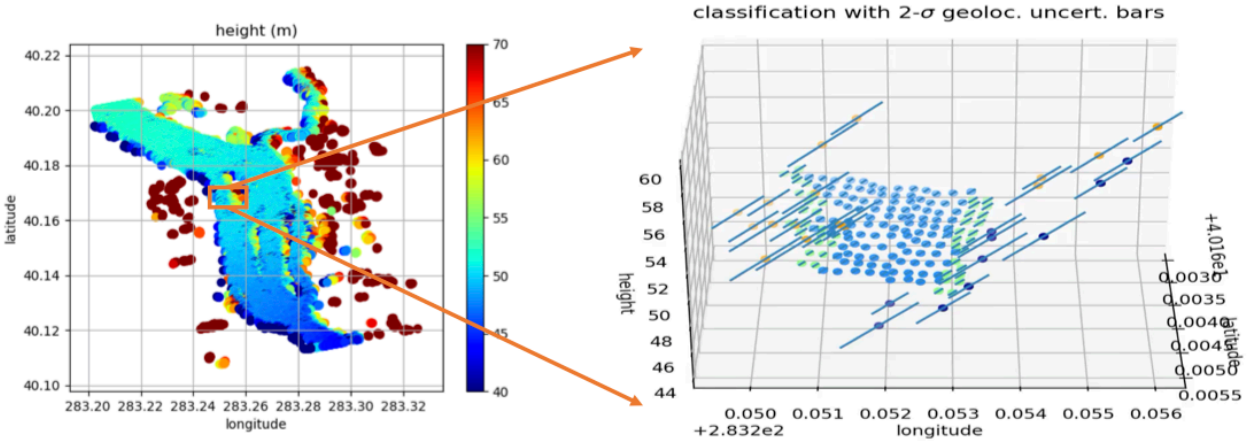

Figure 2. Simulated example of the height from the L2_HR_PIXC product projected into the ground plane (left) and represented as a 3-D point cloud (right).

© 2025 California Institute of Technology. Government sponsorship acknowledged.

2.2 Latency

The L2_HR_PIXC product is generated with a latency of at most 45 days from data collection. The latency allows for consolidation of instrument calibration and the required auxiliary or ancillary data that are needed to generate this product. Different versions of the product may be generated at different latencies and/or through reprocessing with refined input data.

© 2025 California Institute of Technology. Government sponsorship acknowledged.

3 Product Structure

3.1 Granule Definition

The L2_HR_PIXC product is organized into swath-aligned tiles as illustrated in Figure 3 and described in **[4]**. Nominally, these tiles are approximately 64 km long in the along-track direction and cover either the left or right side of the KaRIn swath (~64 km wide from nadir to the far-range swath edge). The left and right half swaths are defined as if standing on the Earth surface facing the direction of the spacecraft velocity vector. These tiles have a one-to-one correspondence with tiles of the Level 1B High Rate Single Look Complex (L1B_HR_SLC) product **[5]**. However, the L2_HR_PIXC tiles do not contain overlap between successive tiles, while the L1B_HR_SLC tiles, which are slightly longer in the along-track direction, do overlap.

Note that the exact cross-track width of the SWOT half swaths on either side of nadir vary due to the manner in which the KaRIn range measurement maps into ground-projected coordinates. This mapping depends on the KaRIn parameters, the orbit, and the topography. Moreover, measurements are only useful where the SNR is sufficiently high. The L2_HR_PIXC product is designed such that no KaRIn measurements are left out of the product simply because they fall outside of granule cross-track boundaries. However, data samples that are not reliable (e.g., due to insufficient SNR) are flagged. This approach preserves the most information and allows users to decide how best to use the data; users are expected to check the data quality flags. The ~64 km cross-track extent of each tile therefore covers more than the typical extent of "good" SWOT measurements. That is, while the SWOT performance requirements apply only from 10 to 60 km from nadir, it is possible for useful measurements to occur between 0 and ~64 km from nadir. Such measurements are reported in the L2_HR_PIXC product as long as they fulfill the nominal criteria for inclusion (no measurements are excluded solely because they lie outside the 10–60 km swath specified by the requirements).

The PIXC tile boundaries remain approximately fixed geographically, following a predefined swath-aligned system described in [4], although the precise boundaries depend on the particular spacecraft position and velocity and the KaRIn pulse timing when the data were collected. The L2_HR_PIXC tile boundaries correspond exactly to the tile boundaries of the L2_HR_PIXCVec product.

The tile boundaries are defined by a set of ideal, geographically fixed reference tile boundaries (see [4]). These reference tiles are numbered sequentially by pass number in the ideal reference orbit repeat cycle, along-track tile number within the pass, and side (left or right). A pass here refers to half of an orbit from extreme south latitudes to extreme north latitudes or vice versa. Along-track tile numbers are numbered sequentially following the spacecraft flight direction, so the tile numbers increase from south to north for ascending passes and from north to south for descending passes.

Note that each sample in a given granule includes enough information to give its absolute geometry and time such that samples from different granules can be related (see Section 4).

© 2025 California Institute of Technology. Government sponsorship acknowledged.

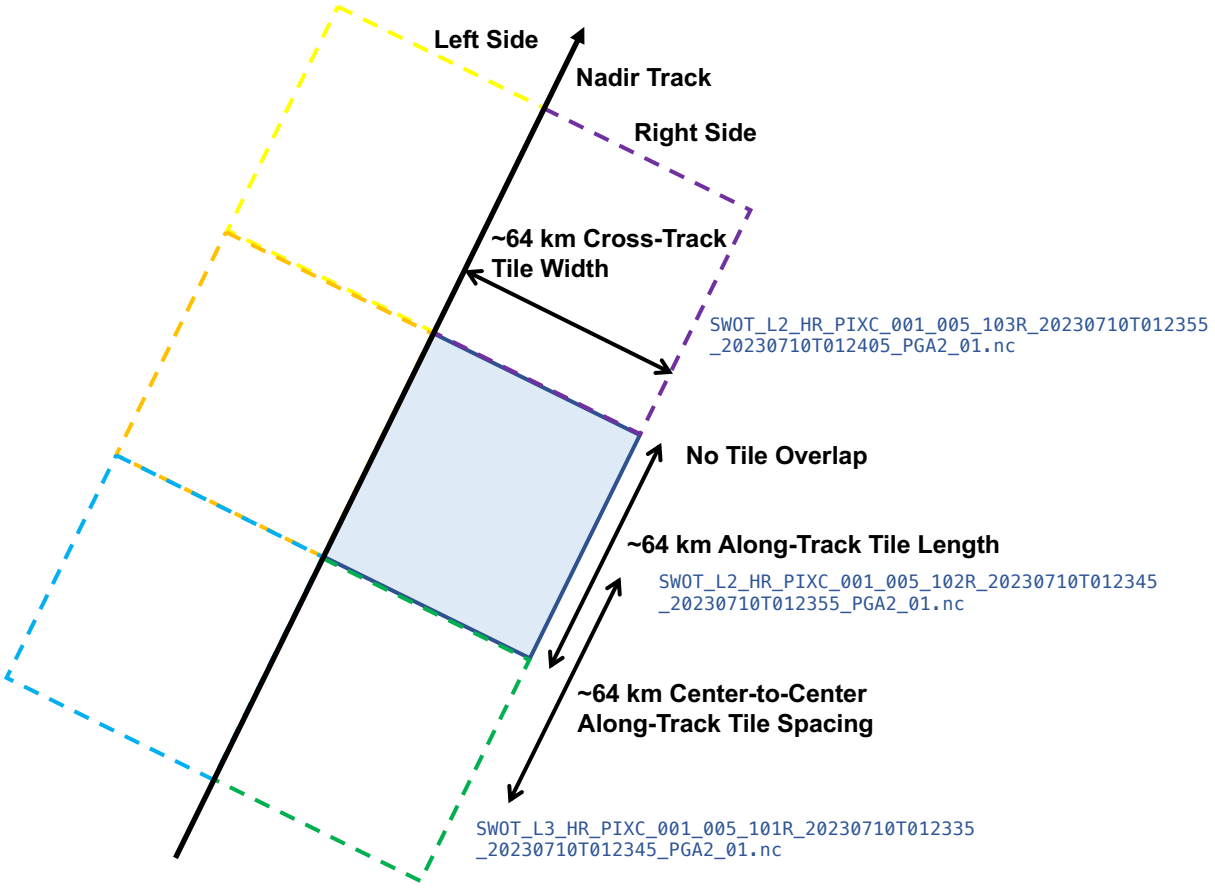

Figure 3. L2_HR_PIXC product granule illustration.

3.2 File Organization

The L2_HR_PIXC science data product adopts the NetCDF-4 file format. It has a section of global attributes and three groups of data: *pixel_cloud*, *tvp*, and *noise*.

Table 1. Description of the file comprising the L2_HR_PIXC product.

File	Name	Description
1	Level 2 KaRIn high-rate water mask pixel cloud product.	Provides Level 2 pixel measurement information, time-varying parameter (tvp) platform information, and noise estimates in separate NetCDF groups.

The *pixel_cloud* group is a collection of 1-D arrays representing the various datasets given for each interferogram pixel detected as water, as well as neighboring pixels and those in the pruning/inclusion mask. The data in the *pixel_cloud* group include the multilooked (spatially averaged) interferogram information, the radiometric calibration (X factor), the detected classification and water fraction estimates, as well as geolocated heights, geolocation sensitivities, various flags, geophysical corrections, and height references (see Section 4.1.2).

© 2025 California Institute of Technology. Government sponsorship acknowledged.

The *tvp* and *noise* groups contain information on the radar position, velocity, attitude, and internal noise. These datasets are given as functions of time and can be associated with samples in the *pixel_cloud* group by multiple variables in the *pixel_cloud* group as described below in Sections 3.5 and 3.6.

Table 2: Description of the NetCDF groups in L2_HR_PIXC product.

Group Name	Description
pixel_cloud	Pixel cloud output for the granule that provides the majority of the information for each spatial sample: height, location, classification, and several other variables.
tvp	This group is essentially a copy of the *tvp* group from the L1B_HR_SLC product [5] from which the pixel cloud product was created. This group contains the sensor position, velocity, attitude, time, and baseline information corresponding to each along-track index.
noise	This group is essentially a copy of the *noise* group from the L1B_HR_SLC product [5] from which the pixel-cloud product was created. This group contains noise estimates in a one-dimensional array that has an entry for each line in the single look complex (SLC) image.

Because there is no native type for a complex floating-point value in NetCDF-4, the 1-D arrays of complex values are represented in the product as 2-D arrays, where the second dimension has a depth of 2 for the real and imaginary parts (the real part is given first) of each complex value. That is, because the real and imaginary parts of array *arr* at indices *m* and *n* cannot be represented as *arr*[*m*][*n*].*real* and *arr*[*m*][*n*].*imag*, the real and imaginary parts are represented as *arr*[*m*][*n*][0] and *arr*[*m*][*n*][1], respectively.

3.3 File Naming Convention

The L2_HR_PIXC product adopts the following file naming convention:

SWOT_L2_HR_PIXC_<CycleID>_<PassID>_<TileID>[L/R]_<RangeBeginningDateTime>_<RangeEndingDateTime>_<CRID>_<ProductCounter>.nc

The <CycleID>, <PassID>, and <TileID> identify the repeat cycle, pass, and tile of the data. The <RangeBeginningDateTime> and <RangeEndingDateTime> provide the UTC time range of data used to derive the data product. The <CRID> above contains the composite release identifier. It contains the version code of the data product, which changes if the processing software and/or auxiliary inputs are updated. The <ProductCounter> identifies the version of product that may have been generated multiple times with the same version of processing software.

An example filename is:

`SWOT_L2_HR_PIXC_001_005_001L_20210612T072103_20210612T072113_PGA2_03.nc`

© 2025 California Institute of Technology. Government sponsorship acknowledged.

3.4 Spatial Sampling and Resolution

In this document, the term “posting” refers to the spatial sampling of a horizontally gridded data set. The term “sampling” is used generically to refer to the manner or locations at which the data are discretized. One individual data value is called a sample. Samples from a 2-D spatial array are often also called “pixels.” The term “azimuth” refers to the along-track dimension, and “range” refers to the slant-range or cross-track dimension of the KaRIn synthetic aperture radar (SAR) SLC images that underlie the pixel cloud. With SLC images represented in a regular 2-D image grid, the along-track and cross-track image indices are sometimes referred to as “lines” and “pixels,” respectively, as illustrated in Figure 4. Note, however, that while the information in the pixel cloud product can be traced from the 2-D SLC images, the pixel cloud samples themselves are not represented in the product as filled 2-D arrays (see below). The usage of the term “pixel” should be evident from context.

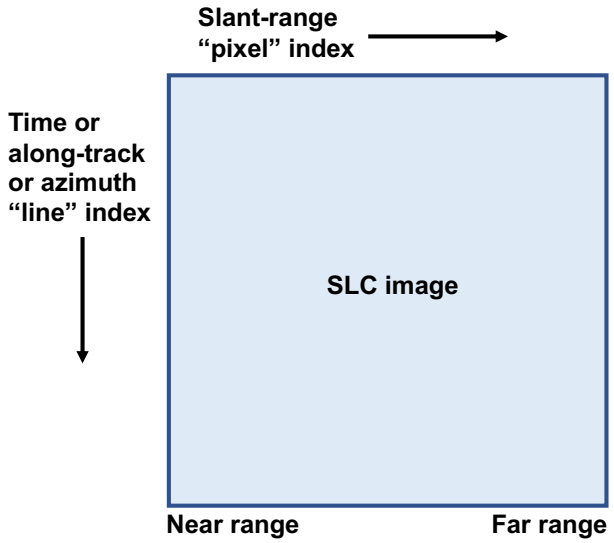

Figure 4. SLC image dimensions.

In order to preserve spatial resolution while allowing enough spatial averaging to reduce noise to desired levels, pixel-cloud processing involves multiple stages of spatial averaging, with different aspects of data processing done at different stages. Data after the first stage of spatial averaging is known as the ‘rare’ layer, while data after the second stage of (adaptive) spatial averaging is known as the ‘medium’ layer (here, a ‘layer’ is a set of variables computed from a given level of spatial averaging—see below). Information from both the rare and medium layers are included in the pixel cloud product, although the product is not strictly organized by layer (i.e., both the rare and medium layers are stored in the same netcdf group). Note that the L2_HR_PIXCVec product applies spatial smoothing at the entire-water-body level and this can be considered as a ‘well-done’ layer, although it is generated as a separate data product.

Note that some along-track spatial averaging and resampling also occurs in the KaRIn instrument itself before the data are downlinked and before SLCs are formed in a process called presumming; the along-track SLC sampling matches the presum sampling of the downlinked HR data. The sampling of the pixel-cloud is thus ultimately derived from KaRIn.

© 2025 California Institute of Technology. Government sponsorship acknowledged.

The posting in the pixel cloud corresponds to the rare interferogram posting. That is, each pixel in the pixel cloud corresponds one-to-one to a particular pixel in the radar interferogram image after azimuth multilooking (i.e., spatial averaging in azimuth) and down-sampling from the SLC posting to obtain approximately four effective independent looks (i.e., approximately four independent realizations are averaged and decimated, giving a nominal along-track ground posting of approximately 22 m, varying slightly over the orbit). Details are available in [1].

However, only a small fraction of the pixels in the interferogram are saved in the pixel cloud (mainly water pixels and pixels in floodplains; see the *classification* variable and [1]). The pixel cloud can be thought of either as a sparse raster (in the 2-D range-azimuth coordinates of the rare interferogram image plane or 'slant plane'), or, equivalently, as an unstructured list of geolocated pixels (in 3-D ground coordinates). Therefore, while much of the pixel-cloud processing is done on 2-D interferogram arrays internally, the output is represented as a 1-D array or list after the samples are pruned to remove pixels that are not expected to contain useful measurement information (i.e. most land surfaces) as well as pixels that are outside the tile granule (since the 2-D image has some overlap with adjacent along-track tiles). Since water occupies only a small fraction of the observed surface area, this considerably reduces the size of the product. Each sample in the 1-D array maintains enough information to determine where the sample was located in the original 2-D slant-plane arrays.

Due to the nonlinearity of height reconstruction and geolocation, some additional multilooking (spatial averaging) is necessary to reduce noise amplification before height reconstruction is performed. For a typical brightness of water in the middle of each half swath, where the signal-to-noise ratio (SNR) is highest, about 40 independent looks are necessary for this purpose. In order to preserve the ability to resolve the boundaries of 50-100 m rivers, this additional multilooking is done adaptively, averaging water and land separately while preserving the rare posting. This results in two layers of smoothing for each pixel in the pixel cloud: the rare layer (~4 effective looks), which preserves resolution (higher spatial-frequency information), and the medium layer (~40 effective looks), which attempts to optimize the noise-versus-resolution trade-off for height reconstruction. This is illustrated in Figure 5.

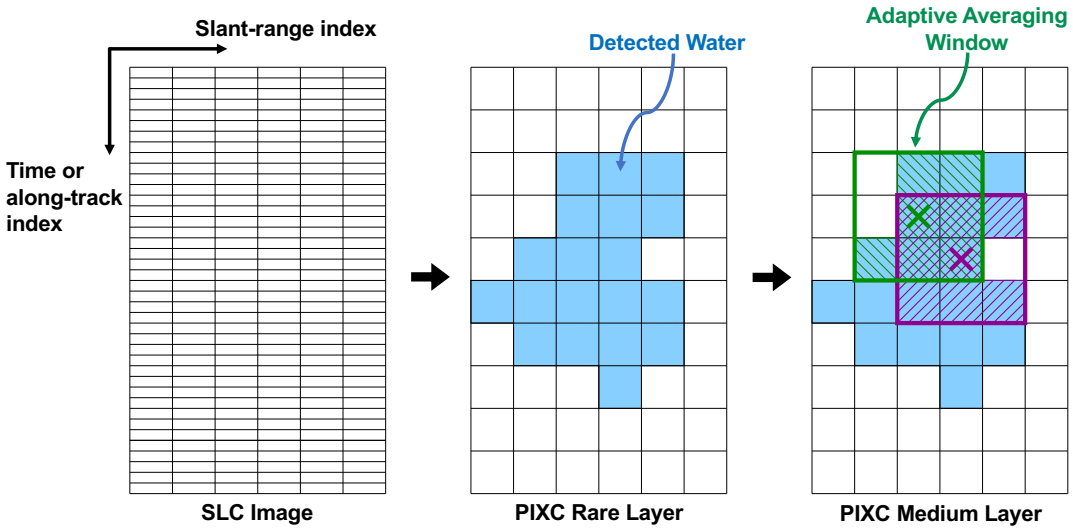

Figure 5. Notional illustration of the relationships between the posting and information content of SLC ("raw"), rare, and medium samples in the slant plane.

© 2025 California Institute of Technology. Government sponsorship acknowledged.

As depicted notionally in Figure 5, several SLC samples are averaged and decimated in the along-track direction (with no change to the slant-range sampling) to obtain the rare layer. The sample marked by the green "X" in the medium layer is formed from the average of all rare interferogram pixels of the same class (detected water, indicated by blue pixels, in this example) within an averaging window indicated by the bold green box; these pixels are indicated by the green diagonal hash. Similarly, the sample marked by the purple "X" is formed from the average of the rare interferogram pixels indicated by the diagonal purple hash. The medium-layer samples indicated by the green and purple "X" markers are hence highly correlated. Note that with a 3 × 3 window, as shown, the number of looks in the medium layer is at most 36 (9 times the 4 effective along-track looks of the rare interferogram relative to the SLC sampling). Note that Figure 5 is provided for illustrative purposes only. See [1] for details on the pixel-cloud algorithms.

It is important to note that the underlying slant-plane grid that defines the sample locations of the medium layer is identical to that of the rare layer because the medium layer cannot generally be decimated without loss of information given the adaptive nature of the medium-layer averaging. Consequently, information in medium-layer pixels can be highly correlated from one sample to the next. One should not expect to obtain $\sqrt{N}$ reduction in the random error after averaging N neighboring medium-layer height values together. Note that all information needed to appropriately compute the noise reduction and aggregate the height uncertainties are reported in the product.

While the rare and medium layers are sampled at identical locations in the slant plane, the additional averaging incorporated into the medium layer gives a more reliable 3-D geolocation. Geolocations for the rare layer would be so noisy (primarily in the height and cross-track dimensions) that they would not be useful at that resolution and, after averaging down such heights to the same resolution as the medium heights, they would be less accurate than the medium heights themselves (because of the non-linearity of the geolocation algorithm). Rare geolocations are hence not given in the product.

Additional aggregation is done during river and lake vector processing, which use the pixel-cloud data product as input, and the companion L2_HR_PIXCVec product is produced to complement the PIXC product (see [3]). The L2_HR_PIXCVec product contains very smoothed heights and geolocations consistent with the river and lake vector products and can be viewed as a third 'well-done' layer. The level of smoothing in this well-done layer significantly reduces the geolocation error (variability) and can be used to obtain an estimate of the shape or outline of the water features. Furthermore, these well-done geolocations better-preserve the neighborhood topology that exists in the slant-plane images.

Note that geophysical corrections and height references are reported for every pixel in the *pixel_cloud* group for simplicity and user convenience. However, these quantities are generally spatially smooth, so they are highly oversampled in the product.

The *tvp* and *noise* groups are posted in the L1B_HR_PIXC product at the original posting and along-track extent as the upstream L1B_HR_SLC product [5] from which they are obtained. That is, both the *noise* and the *tvp* groups are sampled at the along-track spacing of the SLC images, which is finer than the pixel-cloud along-track spacing. They both also extend beyond the along-track coverage of the pixel-cloud granule, with the *tvp* group extending even further beyond along-track extent of the *noise* group. Consequently, along-track sample index *k* in each

© 2025 California Institute of Technology. Government sponsorship acknowledged.

of the *pixel_cloud*, *tvp*, and *noise* groups would correspond to different along-track locations (see Section 3.6 below).

3.5 Temporal Organization

The 1-D arrays of pixel cloud information in the *pixel_cloud* group are stored by scanning the underlying 2-D arrays in row-major order, with rows representing the along-track index (increasing with time or along-track position) and columns representing the slant-range index (increasing with range), and discarding pixels that do not meet the criteria for inclusion in the product. Because the data samples are arranged in the file spatially, they may not be in strict order temporally in the file when the spacecraft attitude is not ideal, however. For example, spacecraft yaw may result in the near-range pixels of a row being illuminated slightly earlier or later than the far-range pixels. The time is reported for each sample, however.

The time of peak illumination for a pixel is defined as the time that the KaRIn antenna boresight passed over the pixel. This time can be thought of as the time that the pixel was observed in the pass, even though the measurement actually involves a finite integration period (corresponding to hundreds of radar pulses), which is approximately centered at the peak illumination time.

A variable called *illumination_time* is reported for each pixel in the *pixel_cloud* group representing the UTC time of illumination (*illumination_time_tai* gives the TAI time for each pixel). The illumination time can be used to look up the sensor information in the *tvp* group (including spacecraft attitude, spacecraft position, and the corresponding spacecraft UTC or TAI times), or to look up noise information in the *noise* group. The *tvp*, *noise* and *pixel_cloud* measurements can also be associated by the relationships between the sampling grids described below in Section 3.6.

The samples of the *tvp* and *noise* groups are given in order of increasing time (equivalent to increasing along-track position).

3.6 Spatial Organization

The samples in the 1-D arrays in the *pixel_cloud* group are given in order of increasing along-track index then increasing slant-range index from the underlying 2-D arrays, though not all pixels in the 2-D arrays are kept in the 1-D arrays. The slant-range and along-track indices of each sample in the *pixel_cloud* group into the underlying 2-D arrays are given in the *range_index* and *azimuth_index* variables. These indices are relative within a granule and cannot necessarily be compared between granules.

The samples of the *tvp* and *noise* groups are given in order of increasing along-track position (equivalent to increasing time), although the *tvp* group covers a greater extent in the along-track dimension than the *noise* group.

The conceptual relationship between the sampling and spatial organization of the *tvp*, *noise*, and *pixel_cloud* groups is illustrated in Figure 6. Note that the TVP, the noise, and the SLC arrays are all sampled at the KaRIn presum echo spacing in azimuth, which is finer than the rare posting of the pixel cloud by *num_azimuth_looks*. The TVP has a greater azimuth extent than either the noise or SLC data. The rare image grid has the same azimuth extent as the SLC and the noise data. Note that the offset of the rare multilooking grid from the SLC grid in azimuth is chosen so that consecutive tiles are seamlessly multilooked (i.e., so that the

© 2025 California Institute of Technology. Government sponsorship acknowledged.

overlapping portions of the rare interferogram variables of two consecutive tiles are identical).

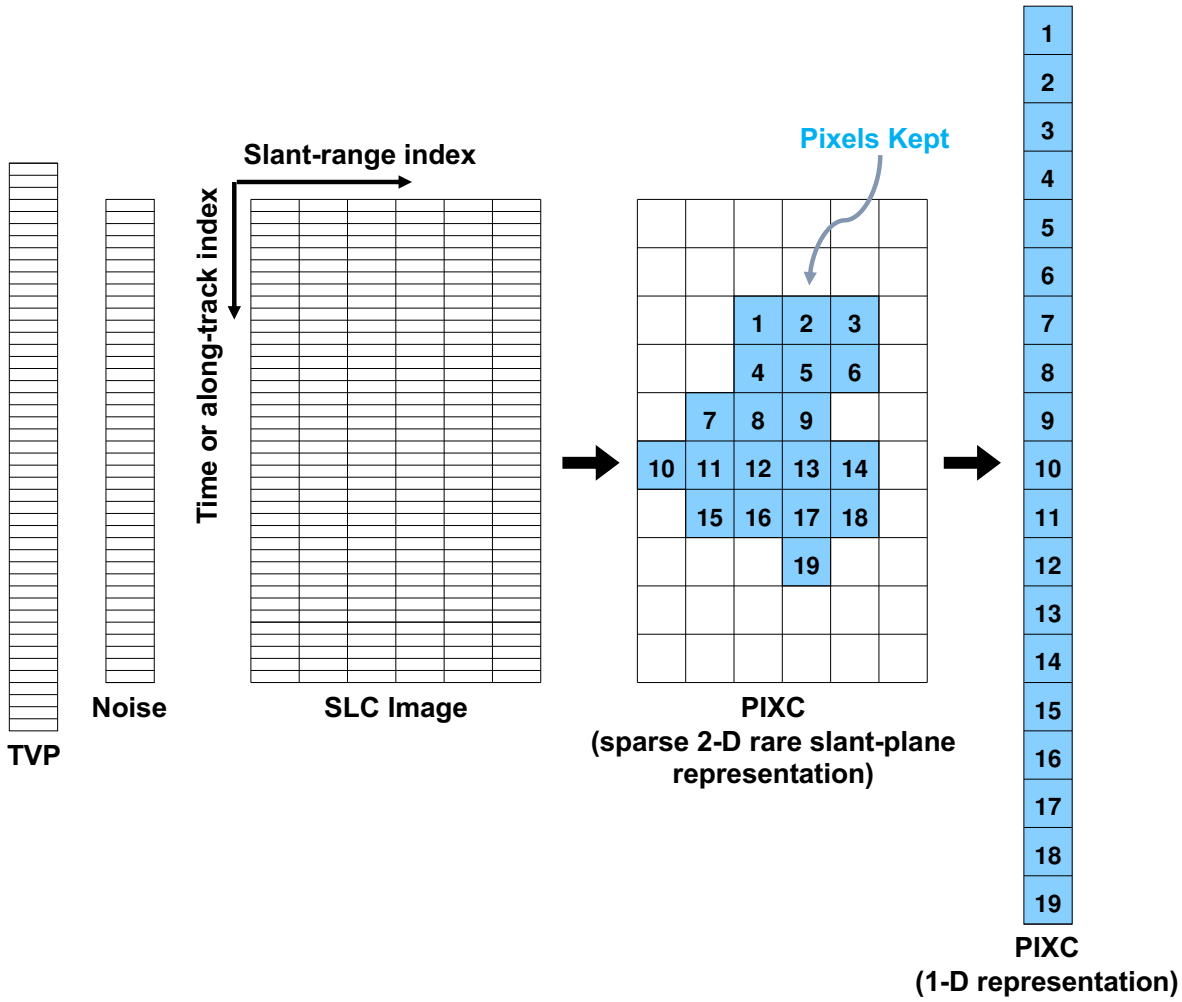

Figure 6. Conceptual illustration of the relationships between the sampling of the *tvp*, *noise*, and *pixel_cloud* groups with respect to the SLC sampling grid.

Conceptually, samples in the *pixel_cloud* group are related to corresponding samples in the *noise* group through the following equation:

$$k_noise = azimuth_index[k_pixel_cloud]*num_azimuth_looks + azimuth_offset$$

where *k_pixel_cloud* is an index into the 1-D arrays of dimension in the *pixel_cloud* group (ranging from 0 to *points*-1) and *k_noise* is an index into the 1-D arrays of dimension in the *noise* group (ranging from 0 to *num_lines*-1), *num_azimuth_looks* is the commanded number of azimuth looks for rare multilooking, and *azimuth_offset* is an azimuth shift that handles the multilooking consistently across tile boundaries.

An index *k_tvp* into a 1-D array for a variable in the *tvp* group (ranging from 0 to *num_tvps*-1) can also be aligned with an index *k_noise* through the global attribute *slc_first_line_index_in_tvp*:

© 2025 California Institute of Technology. Government sponsorship acknowledged.

k_tvp = *k_noise* + *slc_fist_line_index_in_tvp*

Note that for convenience a variable called *pixc_line_to_tvp* (that is equivalent to *k_tvp*) is reported for each rare azimuth line in the product. Using this variable, the TVP and noise indices can also be computed as:

k_tvp = *pixc_line_to_tvp*[*azimuth_index*[*k_pixel_cloud*]]
k_noise = *pixc_line_to_tvp*[*azimuth_index*[*k_pixel_cloud*]] - *slc_fist_line_index_in_tvp*

Note that samples in the *pixel_cloud* group can also be associated with the KaRIn state information when the sample was imaged by matching the time between the *illumination_time_tai* variable in the *pixel_cloud* group with the *time_tai* variable in the *tvp* group. Note, however, that the illumination time may not occur at the TVP line corresponding to *pixc_line_to_tvp* if non-ideal antenna pointing causes the antenna footprint to be slightly ahead of or behind the cross-track direction.

3.7 Volume

Table 3 provides the expected volume of the individual groups comprising the L2_HR_PIXC product. These data volume estimates assume that no NetCDF compression is applied.

The values provided in Table 3 are based on the following assumptions, which represent an expected typical case for volume-estimation purposes:

1. Along-track extent of 64 km, with 22 m along-track posting (approximately 4 effective looks), which corresponds to about 3000 pixels in the along-track direction of the underlying 2-D arrays.
2. 64 km extent for each swath in the cross-track direction, which corresponds to about 4600 single-range-look pixels (this is the approximate length of the full range window; KaRIn performance is generally best near the center of the swath and degrades quickly outside the central 50 km of each half swath).
3. Approximately 10% of the pixels are expected to be kept on average for a given scene. (For reference, an upper-bound on the data volume if 100% of the pixels are kept is also given in Table 3.)

Together this results in 13,800,000 pixels per tile, on average. In the *pixel_cloud* group there are 55 variables with a total of 219 bytes per pixel, plus 2 variables with one sample per azimuth line with a total of 5 bytes. For each tile, this results in 13,800,000*219*0.1+3000*5 = 302.24 MB (max ~3.02 GB if the whole scene is water) for the *pixel_cloud* group.

The *tvp* group has samples in the along-track dimension only. Furthermore, the *tvp* samples are given for every along-track location (not just those that have water), and at the full posting of the SLC image (about 7 times denser than the rare posting) and with overlap at each along-track end of the tile. Note that there are about 21400 along-track samples in the SLC product, but the *tvp* group has additional overlap corresponding to the raw data size resulting in a total of about 21600 samples. There are 24 variables with a total of 174 bytes per along-track index. This results in a group size of 21600*174 = 3.8 MB.

© 2025 California Institute of Technology. Government sponsorship acknowledged.

The *noise* group is reported with one sample per along-track SLC sample, and there are two 4-byte variables giving 21400*8 = 0.2 MB.

Table 3: Description of the data volume of the L2_HR_PIXC product.

Part	Group	Name	Expected Mean Volume (10% water) / Tile (GB)	Maximum Volume (100% water) / Tile (GB)
1	*pixel_cloud*	Pixel Cloud	0.30224	3.0222
2	*tvp*	Time Varying Parameters	0.0038	0.0035
3	*noise*	Noise	0.0002	0.0002
		Total	**0.306**	**3.02**

© 2025 California Institute of Technology. Government sponsorship acknowledged.

4 Qualitative Description

4.1 Level 2 KaRIn HR Pixel Cloud Data File

Several variables in the L2_HR_PIXC product are defined relative to a reference frame that is fixed to the KaRIn instrument called the KaRIn Metering Structure Frame (KMSF), illustrated in Figure 7. This frame is defined with the origin near the middle of the interferometric baseline, with the two antennas along the +*y* and –*y* axes. The +*z* axis of this frame is controlled to point approximately toward nadir, so the *x* axis is approximately parallel or antiparallel to the Earth-relative spacecraft velocity vector. However, the spacecraft periodically performs 180˚ yaw flips (for thermal management reasons, several times per year) such that sometimes the +*x* axis is in the direction of the velocity vector (i.e., satellite flying forward), and sometimes the –*x* axis is in the direction of the velocity vector (i.e., satellite flying backward). Which of the +*y* and –*y* antennas is to the left or right of the spacecraft along-track direction therefore depends on the yaw state of the spacecraft. As elsewhere in this document, "left" and "right" are defined as if standing on the Earth surface and facing the direction of the spacecraft velocity vector.

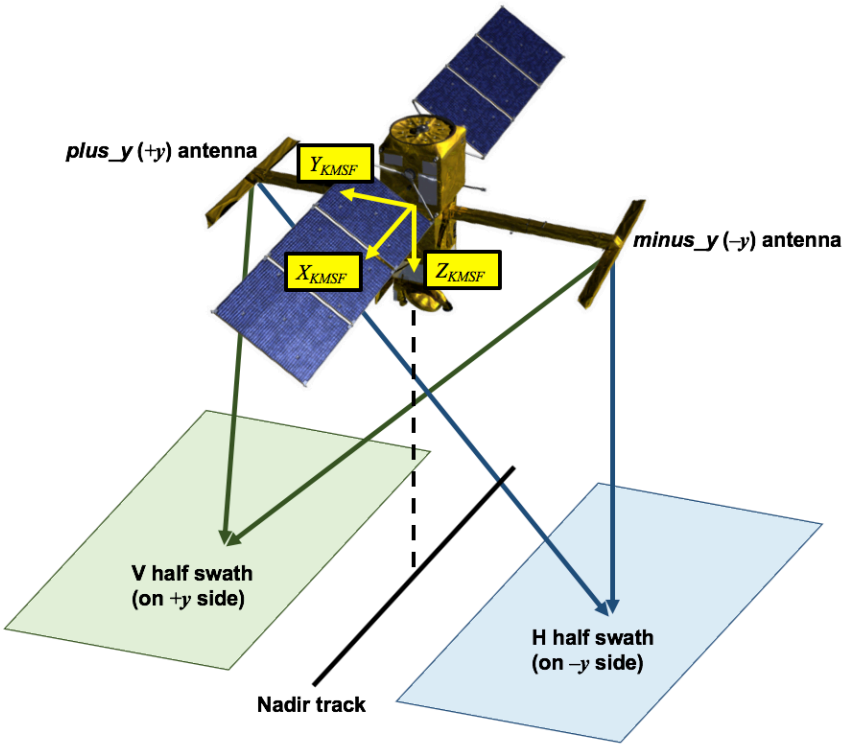

Figure 7. Illustration of the KMSF frame and the polarizations (V and H) of the two KaRIn half swaths. The velocity direction can be along $+X_{KMSF}$ or $-X_{KMSF}$ depending on the yaw state of the spacecraft.

In the L2_HR_PIXC product, variables that are associated with antenna channels are defined with respect to the physical antenna and receiver hardware of the channel (regardless of which side (left or right) of the nadir track the hardware was on given the yaw state of the spacecraft). Following KaRIn instrument conventions, these variables are named with the identifiers "plus_y" and "minus_y" in reference to the antennas on the +*y* and –*y* sides of the KaRIn frame. When the spacecraft yaw (from the *yaw* variable in the *tvp* group) is close to 0˚, the +*y* and –*y*

© 2025 California Institute of Technology. Government sponsorship acknowledged.

antennas are to the right and left, respectively, of the nadir track when facing in the direction of the velocity vector; the opposite is true when the yaw is close to 180˚, which indicates a yaw-flipped state.

As noted above, the left and right half-swaths on the ground are given in separate product tiles; the mapping of how the *+y* and *–y* antennas are used for each of the left and right half swaths is handled during data processing.

The radar signal is horizontally (H) and vertically (V) polarized for the half swaths on the *-y* and *+y* sides of the KaRIn frame, respectively. Therefore, the polarizations for the left and right swaths are H and V, respectively, when the yaw is close to 0˚. The polarization is given by the global attribute *polarization*.

When the KaRIn prime high-power amplifier (HPA) is used, the *+y* antenna transmits regardless of the yaw state. The *–y* antenna transmits when the cold-spare HPA is used (likely only in the event of a failure of the prime unit). Which of the antennas is transmitting is given by the global attribute *transmit_antenna*. A swap to the spare HPA would necessitate recalibration of the instrument, though in principle the swap should eventually be transparent with respect to the primary measurement quantities (geolocation and classification) of the L2_HR_PIXC product. However, users of the complex interferogram information in the product will need to account for the swap in the bookkeeping of their computations.

All variables that give position, velocity, and attitude relative to the Earth frame are defined with respect to the International Terrestrial Reference Frame (ITRF). In this Earth-Centered Earth-Fixed (ECEF) frame, the *+z* axis frame goes through the north pole, and the *+x* axis goes through both the equator (zero latitude) and the prime meridian (zero longitude).

All variables that are defined with respect to a reference ellipsoid assume the reference ellipsoid parameters that are given in the global attributes (*ellipsoid_semi_major_axis* and *ellipsoid_flattening*) of the product file itself.

4.1.1 Global Attributes

A complete list of global attributes is given in Table 6. In addition to common global attributes, several global attributes give information that describe the spatial sampling of the KaRIn measurement and its interpretation:

- *wavelength*: Wavelength corresponding to the effective radar carrier frequency that should be used for height reconstruction after accounting for spectral shifts and filtering.
- *near_range*: Slant range to the first range bin in the underlying 2-D arrays upon which the 1-D pixel cloud samples are taken. Changes to the KaRIn starting range are compensated during ground processing so that the near-range value of the pixel cloud data is constant within a tile (but varying from tile to tile).
- *nominal_slant_range_spacing*: Spacing between range samples in the underlying 2-D arrays upon which the 1-D pixel cloud samples are taken.
- *time_coverage_start*, *time_coverage_end*: UTC times that the first and last measurements in the granule were collected.
- *polarization*: Flag indicating whether the tile is observed with a horizontal (H) or

© 2025 California Institute of Technology. Government sponsorship acknowledged.

vertical (V) signal polarization. The KaRIn V half-swath is always on the +*y* side of the spacecraft, which is to the right of the nadir track if the yaw is near zero (or to the left if the yaw is near 180˚). The KaRIn H half swath is always on the -*y* side of the spacecraft, which is to the left of the nadir track if the yaw is near zero (or to the right if the yaw is near 180˚).

- *transmit_antenna*: Flag that indicates which of the KaRIn antennas (plus_y or minus_y) is transmitting.
- *processing_beamwidth*: Angular extent of the synthetic aperture from a ground target. This parameter determines the single-look along-track resolution of the KaRIn measurement and is hence related to the posting and the effective number of independent looks.
- *slc_along_track_resolution*: Effective along-track resolution to compute the equivalent (effective) number of independent looks when spatially averaging samples at the SLC posting.
- *slc_range_resolution*: Effective slant-range resolution to compute the equivalent (effective) number of independent looks when spatially averaging samples at the SLC posting.
- *slc_first_line_index_in_tvp*, *slc_last_line_index_in_tvp*: Indices in the 1-D TVP array of the first and last SLC image lines from which the pixel cloud was formed. These give information on the along-track extent of the SLC images input to pixel-cloud processing. These index values start from 0.

4.1.2 Pixel Cloud Group Data

The *pixel_cloud* group contains the majority of the data commonly thought of as being in the pixel cloud, with information that varies spatially with measurement location on the ground. The variables associated with pixel cloud samples can be thought of conceptually as belonging to "rare" and "medium" layers, which are defined by the level of spatial averaging that has been applied, as described in Section 3.4. A "well-done" layer is available in the L2_HR_PIXCVec product [3].

Note that the rare and medium layers are comprised of sets of variables in the *pixel_cloud* data group, but there are not explicit NetCDF subgroups in the product for the rare and medium layers. That is, variables in the rare and medium layers both reside in the same (*pixel_cloud*) group rather than in subgroups for each layer.

4.1.2.1 Pixel Cloud Group Attributes

The following parameters are provided as group attributes to the *pixel_cloud* group:

- *interferogram_size_azimuth, interferogram_size_range*: Gives the size (i.e., the maximum range and azimuth indices from 1) for the underlying 2-D image arrays of the KaRIn measurement after azimuth downsampling to form the rare and medium grids, which are identical to one another, before samples are pruned and converted into the 1-D pixel-cloud arrays. Note that *interferogram_size_azimuth* applies to the along-track extent of the 2-D image arrays before overlapping pixels between SLC tiles are discarded. The *pixc_line_qual* variable indicates which lines are considered part of the current (non-overlapping) output PIXC tile.

© 2025 California Institute of Technology. Government sponsorship acknowledged.

- *looks_to_efflooks*: A scalar that indicates the ratio (in the limit) between the number of actual samples and the effective number of independent samples during spatial averaging over a large 2-D area. This value is typically greater than 1. The effective number of independent looks (either *eff_num_rare_looks or eff_num_medium_looks*) can be multiplied by this number in order to obtain the approximate number of real looks. This factor relates to uncertainty estimation.
- *num_azimuth_looks*: A scalar that indicates the number of looks commanded in the rare multilooking. The actual number of rare looks taken may differ from *num_azimuth_looks* due to how flags and missing data are handled in the multilooking algorithm.
- *azimuth_offset*: A zero-base index indicating the azimuth offset applied in the rare multilooking which is chosen so that the overlapping portion of the 2D interferogram images for consecutive tiles (before pruning) are consistent. This value also includes an integer offset of half the commanded number of looks (rounded down) so that a given rare pixel index gets mapped back to the presum-posted index nearest the center of the rare pixel (rather than the beginning).

4.1.2.2 Rare Layer

The rare layer of the *pixel_cloud* group contains information that is computed for pixel cloud samples after an initial (rare) along-track multilooking operation and subsequent downsampling but before additional adaptive averaging (medium). For this layer, no geolocation is given because the geolocation is too noisy to be useful for most applications without additional averaging (which is more beneficial before geolocation, as with the medium layer). This layer is intended for use by expert users who intend to examine the details of how the downstream pixel-cloud results were computed. Such users may wish to process, multilook, and geolocate the rare data for themselves in order to obtain results that are more specifically tailored to their own needs.

The complex interferogram and the corresponding channel powers after rare-layer averaging are given by the following variables:

- *azimuth_index*, *range_index*: Indices of the pixel cloud sample in the 2-D interferogram array (after down-sampling to form the rare layer) upon which the measurement was based. Azimuth refers to the along-track dimension, and range refers to the slant-range or cross-track dimension. These indices are not necessarily applicable across different granules, although the product contains enough information to relate samples across granules by their absolute geolocation and/or their absolute imaging-geometry parameters (see the global attributes *near_range* and *nominal_slant_range_spacing*, the *illumination_time* variable, and the information in the *tvp* group). These index values start from zero.
- *interferogram*: Complex interferogram values stored as 2-D arrays with the real and imaginary components in the fastest-varying (i.e., memory-contiguous) array dimension (the real component is first). These are the rare interferogram measurements without the flattening introduced by the reference interferogram [1]. The phase of the interferogram is related to the true look vector to the target via the viewing geometry. The magnitude is scaled such that it is consistent with the power measurements (*power_plus_y*, *power_minus_y*) in the sense that the coherence can be

© 2025 California Institute of Technology. Government sponsorship acknowledged.

computed as the magnitude of the interferogram divided by the square root of the product of the two channel powers.

- *power_plus_y*, *power_minus_y*: Powers of the two KaRIn channels comprising the interferogram. The powers are given in arbitrary linear units that can be related to the surface reflectivity through the X factor (*x_factor_plus_y*, *x_factor_minus_y*).
- *coherent_power*: Power estimate that represents the coherent combination of the two channel powers. This quantity can be thought of as being computed by rotating the phase of one of the channels with respect to the other using the expected phase difference as obtained by a reference DEM. This approach can produce a power estimate with up to 3 dB SNR gain over the incoherent combination of the powers. Note that if the reference phase is very bad there is the risk of attenuating the power signal. Therefore, the coherent power is filtered in such a way as to make the SNR gain generally greater than or equal to 1, without significantly distorting the distribution. The coherent power is given in linear units that are scaled equivalently to the power.
- *x_factor_plus_y*, *x_factor_minus_y*: Radiometric calibration X factor for the +*y* and the –*y* channels which can be used to map power to sigma0 or normalized radar cross section (NRCS): sigma0 = [power – noise]/x_factor. The X factor is given in linear units.

Information associated with the pixel classification, which is computed from the rare layer and used in downstream pixel-cloud processing, is given in the following variables:

- *water_frac*, *water_frac_uncert*: Water fraction estimate, and its associated uncertainty. This is a noisy estimate of the portion of the pixel that is water. It is nominally between 0 and 1, but because of noise it can be greater than 1 or less than zero. This should not be used directly on each pixel because it is too noisy, but can be beneficial after sufficient averaging/aggregation (e.g., to entire water features). Note that values less than 0 and greater than 1 are not clipped to 0 and 1 in order to avoid bias when aggregating over many pixels. The uncertainty indicates the dispersion of the water fraction estimate (e.g., standard deviation of the distribution of the noisy water fraction estimate).
- *classification*: Multivalued flag that includes values for detected water, dark water, low coherence but bright water, and the corresponding edge/boundary classes.
- *false_detection_rate*, *missed_detection_rate*: Water detection rates that can be used to indicate uncertainty on water detection.
- *prior_water_prob*: Probability of water occurring (between 0 and 1) for this pixel from a prior water mask.
- *prior_water_change*: Normalized value that qualitatively indicates the long-term change in the probability of water based on prior data (positive values indicate increasing probability).
- *bright_land_flag*: Flag indicating that the pixel is an area that is not typically water but that might be expected to be radar reflective (based on prior knowledge). A separate flag value indicates if different sources of prior information conflict with one another. The flag may be used during generation of downstream products or during data analysis to assist in excluding pixels for which false water detections might have occurred.

© 2025 California Institute of Technology. Government sponsorship acknowledged.

- *layover_impact*: Continuous value indicating an estimate of the height error due to layover. This quantity is not likely to be useful on a pixel-by-pixel basis, but may help augment the height uncertainty in the downstream aggregated products.

The effective number of independent raw samples at the SLC posting that are averaged together to obtain the rare layer is given as well:

- *eff_num_rare_looks*: Effective number of independent samples averaged together in azimuth to form the rare layer. The actual number of real looks is generally greater than this value due to oversampling of the SLC samples and can be computed as *eff_num_rare_looks * looks_to_efflooks*. This value is not necessarily an integer. Furthermore, this value may differ from pixel to pixel and from the *num_azimuth_looks* attribute that represents the number of looks that was commanded because of how flags and missing data are handled in the rare multilooking algorithm.

4.1.2.3 Medium Layer

The medium layer of the *pixel_cloud* group contains information that is computed for pixel cloud samples after shape-adaptive averaging of the rare layer based on the detected water mask. This layer is intended for expert users who intend to use the highest resolution heights or geolocation information available from SWOT HR products. It is expected to be the primary layer for most applications of the L2_HR_PIXC product. This layer provides the quantities needed to produce the downstream river, lake, and raster products. Users may wish to work with the medium data for applications where the finest resolution of surface water elevation data is needed in order to obtain results that are more specifically tailored to their own needs than the river, lake, or raster products.

Geolocations are given for all pixels kept in the pixel cloud (not just detected water). The geolocations may be too noisy to be meaningful for some pixels (e.g., dark pixels), as indicated by flags.

- *latitude*, *longitude*: Coordinates giving the horizontal location of the observed pixel as determined by the 3-D geolocation of the processed KaRIn measurement after medium-layer averaging. The latitude is a geodetic latitude with respect to the reference ellipsoid, whose parameters are given in the global attributes of the product (*ellipsoid_semi_major_axis* and *ellipsoid_flattening*). Positive latitude values increase northward from the equator. Positive longitude values increase eastward from the prime meridian.
- *height*: Height of the observed pixel as determined by the 3-D geolocation of the processed KaRIn measurement after medium-layer averaging. The height is given with respect to the reference ellipsoid, whose parameters are given in the global attributes of the product. The reported height is after correcting the measured range for instrument calibrations and signal propagation delays due to the ionosphere and the dry and wet components of the troposphere, as well as crossover calibration (*height_cor_xover).* These applied corrections affect the estimation of the height of the Earth surface with respect to an Earth-centered, Earth-fixed frame. Model-based estimates of tides (solid Earth, load, and pole) and geoid variations are provided in this product, but they have not been applied to the reported value of *height*. For

© 2025 California Institute of Technology. Government sponsorship acknowledged.

example, the value of *height* in the pixel-cloud product for a fiducial marker on the ground would be expected to vary from one SWOT observation to the next due to solid-Earth, load, and pole tides. Similarly, values of *height* over the surface of a large lake in the pixel-cloud product would be expected to show variations that follow the geoid.

- *cross_track*: Approximate cross-track location of the pixel (i.e., distance from the nadir track). This value is reported as a signed distance to the right of the spacecraft nadir point; negative values indicate that the pixel is on the left side of the nadir track. The distance is computed using a local spherical Earth approximation. The distance corresponds to the pixel reference location based on the reference digital elevation model (DEM), not the computed geolocation.
- *pixel_area*: Horizontal area on the ground corresponding to the pixel posting, which is generally smaller than the resolution (i.e., the pixel area does not correspond to the 3 dB width of point target response). This area is defined with respect to the reference DEM, but does not account for surface slopes (i.e., it is the area of a flat surface at the reference height of the pixel).
- *inc*: Incidence angle, which is the angle of the look vector with respect to the local "up" direction where the look vector intersects the reference DEM. The incidence angle is between 0 and 90˚.

Information with which to compute measurement uncertainties is given in the form of underlying observation uncertainties as well as sensitivities of the processed measurements to the underlying observation uncertainties. Therefore, uncertainties can be propagated with proper accounting for the correlations of samples in downstream processing. Uncertainties on the medium-layer geolocations are not given explicitly because it is not expected that these geolocations will be used directly without further aggregation that would necessitate uncertainty propagation.

- *phase_noise_std*: Estimate of the phase noise standard deviation after adaptive averaging to form the medium layer. This estimate of the phase noise is computed analytically from the estimate for the interferometric coherence. Note that phase values are given in radians (not degrees) in the product.
- *dlatitude_dphase*, *dlongitude_dphase*, *dheight_dphase*: Linearized sensitivities of the geolocation with respect to variations in the interferogram phase. Note that phase values are given in radians (not degrees) in the product, so the units of these quantities are degrees of north latitude per radian of phase, degrees of east longitude per radian of phase, and meters of height per radian of phase.
- *dheight_droll*, *dheight_dbaseline*, *dheight_drange*: Linearized sensitivities of the height with respect to variations in the spacecraft roll angle, KaRIn physical baseline length, and absolute range.
- *darea_dheight*: Linearized sensitivity of pixel area to height.

The illumination time of the pixel is the time (quantized to the nearest KaRIn pulse echo) of the center of the synthetic aperture used to focus the SLC SAR images in azimuth. This is intended to correspond to the time of peak illumination by the KaRIn antennas as well as possible, although irregularities in the antenna patterns, misalignments, and calibration errors may make the exact peak illumination time differ slightly.

© 2025 California Institute of Technology. Government sponsorship acknowledged.

- *illumination_time*: Pixel illumination time in UTC time scale (seconds since January 1, 2000 00:00:00 UTC, which is equivalent to January 1, 2000 00:00:32 TAI)
- *illumination_time_tai*: Pixel illumination time in TAI time scale (seconds since January 1, 2000 00:00:00 TAI, which is equivalent to December 31, 1999 23:59:28 UTC)

The variable *illumination_time* has an attribute *tai_utc_difference*, which represents the difference between TAI and UTC (i.e., total number of leap seconds) at the time of the first measurement record in the product group.

- *illumination_time_tai[0] = illumination_time[0] + tai_utc_difference*

The above relationship holds true for all measurement records unless an additional leap second occurs within the time span of the product group. To account for this, the variable *illumination_time* also has an attribute named *leap_second*, which provides the date at which a leap second might have occurred within the time span of the product granule. The variable *illumination_time* will exhibit a jump when a leap second occurs. If no additional leap second occurs within the time span of the product granule *illumination_time:leap_second* is set to "0000-00-00T00:00:00Z".

The table below provides some examples for the values of *illumination_time*, *illumination_time_tai*, and *tai_utc_difference*. With this approach, the value of *illumination_time* will have a 1 second regression during a leap second transition, while *illumination_time_tai* will be continuous. That is, when a positive leap second is inserted, two different instances will have the same value for the variable *illumination_time*, making *illumination_time* non-unique by itself; the difference between *illumination_time* and *illumination_time_tai*, or the *tai_utc_difference* and *leap_second* fields, can be used to resolve this. Some examples are provided in the table below.

UTC Date	TAI Date	time	time_tai	tai_utc_difference
January 1, 2000 00:00:00	January 1, 2000 00:00:32	0.0	32.0	32
December 31, 2016 23:59:59	January 1, 2017 00:00:35	536543999.0	536544035.0	36
December 31, 2016 23:59:59.5	January 1, 2017 00:00:35.5	536543999.5	536544035.5	36
December 31, 2016 23:59:60	January 1, 2017 00:00:36	536543999.0	536544036.0	37
January 1, 2017 00:00:00	January 1, 2017 00:00:37	536544000.0	536544037.0	37
January 1, 2017 12:00:00	January 1, 2017 12:00:37	536587200.0	536587237.0	37

Additional pixel information is given below:

- *eff_num_medium_looks*: Effective number of independent samples at the SLC posting that are averaged together to obtain the medium-layer estimates. Only rare samples of the same class over a sliding window are averaged together, so the number varies per pixel. This value is not necessarily an integer.
- *sig0*: Normalized radar cross section (NRCS) or sigma0. This radar backscatter estimate is derived from the rare interferogram and is given in linear units (not decibels). The value may be slightly negative due to errors in noise estimation and subtraction.
- *sig0_uncert*: Uncertainty estimate of the normalized radar cross section (NRCS) or sigma0. This uncertainty estimate is derived from knowledge of the distribution of the received power and the noise measurements. It represents the 1-sigma uncertainty

© 2025 California Institute of Technology. Government sponsorship acknowledged.

of the measurement and does not include estimates of the uncertainty in the calibration parameters.

- *phase_unwrapping_region*: Index of the region that this pixel was part of during spatial phase unwrapping. The index numbering is arbitrary. This information should only be used to infer whether different pixels were in the same region (i.e., they have the same region index).

As described in the context of the *height* variable, several corrections are applied to the measurements during processing to obtain the reported height values. These correction values are reported so that expert users can gain insight into the ways that raw instrument measurements were combined with calibration factors and external model information. Corrections are given in the product following the sign convention that the reported correction term is added to an uncorrected value to obtain the corrected value.

- *instrument_range_cor*, *instrument_phase_cor*, *instrument_baseline_cor*: Bulk corrections that have been applied to the range, phase, and baseline length to obtain the geolocated results of the medium layer starting from the information in the rare layer. These variables give the additional information that was used to geolocate that is not already embodied in the interferogram and TVP data in the pixel-cloud product. These corrections are interpolated during various levels of processing to reference locations based on the reference digital elevation model (DEM). Each of these corrections are the sum of all corrections applied, though they are applied at different stages of processing and potentially interpolated to different reference locations. The *instrument_range_cor* correction is derived from the media range delay and crossover calibration timing offset, applied directly as a range shift. The *instrument_phase_cor* correction is derived from the media phase shift and crossover calibration phase drift. The *instrument_baseline_cor* is the baseline dilation correction derived from crossover calibration data. As they include the contributions from media delays and crossover corrections, which are reported in separate variables as well, these corrections are complete and sufficient for an expert user to do special processing on the rare interferogram and properly geolocate the result.
- *sig0_cor_atmos_model:* 2-way atmospheric radiometric correction to the sig0 and the X factor, applied as a scale factor in linear units (or equivalently additive in dB). The correction is obtained from a numerical weather prediction model (e.g., ECMWF). This correction is applied to the *x_factor_minus_y* and *x_factor_plus_y* variables before computing the *sig0* quantity so that all of these variables incorporate the correction. The user can remove this correction by a dividing the linear sig0 (and/or *x_factor_minus_y*, and/or *x_factor_plus_y*) by *sig0_cor_atmos_model*, or the user can replace the correction by dividing it out and multiplying by a new correction.
- *height_cor_xover*: Height correction to *height* computed from a combination of sea surface height crossovers between KaRIn/KaRIn measurements and KaRIn/nadir altimeter measurements on different passes within a temporal window surrounding the height measurement. This correction provides an estimate of residual errors that have not been removed with use of ancillary attitude and calibration data during processing. The correction is applied before geolocation, but it is reported in the product as an equivalent height correction. The correction term should be subtracted from the reported pixel height to obtain the uncorrected pixel height.

© 2025 California Institute of Technology. Government sponsorship acknowledged.

Corrections due to propagation delays from the wet troposphere, the dry troposphere, and the ionosphere are applied during data processing. The reported pixel height, latitude, and longitude are computed after adding corrections for these propagation delays to the uncorrected range along slant-range paths. The corrections account for the differential delay between the two KaRIn antennas. These corrections are reported in the product, however, as equivalent vertical path corrections (rather than slant-path corrections) that are computed by applying obliquity factors to the slant-path correction values so that the values in the products can be directly applied to the reported height if desired. The additional path delay relative to free space results in a negative correction value that is added as a correction to the uncorrected range. However, a decrease in the measured range gives an increase in the measured height. Consequently, adding the reported correction terms to the reported pixel height results in the uncorrected pixel height. Model-based corrections are based on SWOT-independent information from the European Centre for Medium-Range Weather Forecasts (ECMWF) and Jet Propulsion Laboratory (JPL) Global Ionosphere Maps (GIM).

- *model_dry_tropo_cor*: Model-based equivalent vertical dry tropospheric path delay correction. This value is computed using surface pressure from the ECMWF numerical weather model.
- *model_wet_tropo_cor*: Model-based equivalent vertical wet tropospheric path delay correction. This value is computed from the ECMWF numerical weather model.
- *iono_cor_gim_ka*: Equivalent vertical ionospheric path delay correction from the JPL Global Ionosphere Maps (GIM) for the KaRIn Ka-band signal.

Geophysical model values are included in the product for downstream use, but they are not used to compute the measured heights reported in the L2_HR_PIXC product (these are not treated as corrections in this product). The sign convention of tide terms is such that a positive tide value gives a greater measured height than a negative tide value. The geoid height is given with respect to the reference ellipsoid whose parameters are defined in the global attributes of the product.

- *geoid*: Model for geoid height above the reference ellipsoid whose parameters are given in the global attributes of the product. The geoid model is EGM2008 [6]. The geoid model includes a correction to refer the value to the mean tide system (i.e., it includes the zero-frequency permanent tide).
- *solid_earth_tide*: Model for the solid Earth (body) tide height. The reported value is calculated using Cartwright/Taylor/Edden [7] [8] tide-generating potential coefficients and consists of the second and third degree constituents. The permanent tide (zero frequency) is not included.
- *load_tide_fes*: Model for geocentric surface height displacement from the load tide. The value is from the FES2022b model [9].
- *load_tide_got*: Model for geocentric surface height displacement from the load tide. The value is from the GOT4.10c ocean tide model [10].
- *pole_tide*: Model for the surface height displacement from the geocentric pole tide. The value is the sum total of the contribution from the solid-Earth (body) pole tide height [11], and a model for the load pole tide height [12]. The value is computed using the reported Earth pole location after correction for a linear drift [13]: in

© 2025 California Institute of Technology. Government sponsorship acknowledged.

milliarcsec,

$$Xp = 55.0 + 1.677dt$$

$$Yp = 320.5 + 3.46dt$$

where *dt* is the time in years since 2000.0.

- *ancillary_surface_classification_flag*: Surface type at the location of the KaRIn measurement derived from a surface classification map that has been built from MODIS and GlobCover [14] data. The flag values have meanings as follows: 0 = open ocean, 1= land, 2 = continental water, 3 = aquatic vegetation, 4 = continental ice or snow, 5 = floating ice, and 6 = salted basin.

The *interferogram_qual* flag indicates the quality of the interferogram quantities in the pixel cloud data (e.g., the *interferogram*, *power_plus_y*, *power_minus_y*, and *coherent_power* variables). There is one value per pixel in the pixel cloud. The flag should nominally be zero; a nonzero flag value indicates either suspect or bad data quality. The various bits of the flag indicate specific information on why the flag may be suspect or bad (see Appendix B for details).

- *interferogram_qual*: Flag that indicates the quality of the interferogram quantities in pixel-cloud data.

The *classification_qual* flag indicates the quality of the classification-related quantities in the pixel cloud data (e.g., the *classification*, and *water_frac* variables). There is one value per pixel in the pixel cloud. The flag should nominally be zero; a nonzero flag value indicates either suspect or bad data quality. The various bits of the flag indicate specific information on why the flag may be suspect or bad (see Appendix B for details).

- *classification_qual*: Flag that indicates the quality of the classification quantities in the pixel-cloud data.

The *geolocation_qual* flag indicates the quality of the geolocation-related quantities in the pixel cloud data (e.g., the *height*, *latitude*, and *longitude* variables). There is one value per pixel in the pixel cloud. The flag should nominally be zero; a nonzero flag value indicates either suspect or bad data quality. The various bits of the flag indicate specific information on why the flag may be suspect or bad (see Appendix B for details).

- *geolocation_qual*: Flag that indicates the quality of the geolocation quantities in the pixel-cloud data.

The *sig0_qual* flag indicates the quality of the sig0 variable in the pixel cloud data. There is one value per pixel in the pixel cloud. The flag should nominally be zero; a nonzero flag value indicates either suspect or bad data quality. The various bits of the flag indicate specific information on why the flag may be suspect or bad (see Appendix B for details).

- *sig0_qual*: Flag that indicates the quality of the sig0 variable in the pixel-cloud data.

The *pixc_line_qual* flag indicates the quality (or availability) of data for water detection during processing. There is one value per cross-track line of pixels in the internal 2-D rare interferogram layer (see Figure 5 and the *azimuth_index* variable). Where pixels from the 2-D rare interferogram are not kept in the L2_HR_PIXC product, *pixc_line_qual* provides information on whether those pixels were discarded because water was not believed to be present, or because the underlying interferogram data were missing or invalid (for example, if HR data were not collected there). The *pixc_line_qual* flag also provides information about

© 2025 California Institute of Technology. Government sponsorship acknowledged.

which lines of the rare radar grid were explicitly excluded because they are outside the tile granule boundary. That is, the rare radar grid extent in azimuth overlaps among consecutive tiles, but the pixels kept in the pixel cloud data do not overlap between tiles. The various bits of the flag indicate specific information on why the flag may be suspect or bad (see Appendix B for details).

- *pixc_line_qual*: Flag that indicates quality (or availability) of an entire cross-track line of pixels in the rare interferogram.

The *pixc_line_to_tvp* variable maps the rare radar grid azimuth line to the TVP index. There is one value per cross-track line of pixels in the internal 2-D rare interferogram layer (see Figure 5 and the *azimuth_index* variable). This quantity handles the offset difference as well as the posting difference between the TVP sampling rare (or medium) radar grid posting. Note that *pixc_line_to_tvp* is the TVP index for which the pixel cloud samples at a given radar grid azimuth index were at broadside, not the TVP index that corresponds to peak illumination by the antenna (as discussed in Section 3.6).

- *pixc_line_to_tvp*: Pixel cloud rare radar grid line index to TVP index mapping.

The *data_window_first_valid* and *data_window_last_valid* variables indicate for each rare/medium azimuth line the indices (see *range_index*) of the first and last bins in the range direction where data may be valid. The KaRIn receiver is commanded to receive echoes only over a short time extent for each radar pulse, and the delay of this commanded receive window varies with topography. For tiles where there is significant topography, the range window can vary significantly over the along-track extent of the tile, and the number of out-of-window slant-plane pixels can be large. Pixels outside the bounds indicated by the *data_window_first_valid* and *data_window_last_valid* variables are not included in the product. These two variables indicate whether pixels at near and far ranges are excluded because they are outside the range window and hence have no valid KaRIn data (as opposed to being in the range window but excluded because water was not detected). The approximate cross-track distances for the first (shortest range) and last (longest range) valid pixels are also reported in the *data_window_first_cross_track* and *data_window_last_cross_track* variables. These two variables provide information about the valid data window pixels as projected into ground coordinates, although the projection at near range may not be very accurate given the steep incidence angles involved. Like the *cross_track* variable, the cross-track distance is defined to be negative to the left of nadir and positive to the right of nadir.

- *data_window_first_valid*: Pixel cloud data window starting index of the first valid pixel in the range direction.
- *data_window_last_valid*: Pixel cloud data window ending index of the last valid pixel in the range direction.
- *data_window_first_cross_track*: Pixel cloud data window starting cross-track distance in meters of the first valid pixel in the range direction.
- *data_window_last_cross_track*: Pixel cloud data window ending cross-track distance in meters of the last valid pixel in the range direction.

4.1.3 TVP Group Data

The *tvp* group contains platform and radar system parameters as a function of time, including

© 2025 California Institute of Technology. Government sponsorship acknowledged.

the spacecraft position, velocity and attitude, as well as the lever arm information of the two antennas comprising the KaRIn interferometer. See Figure 7 and its associated description for the definition of the KMSF frame.

4.1.3.1 Time

Time tags for each TVP data record are provided in the UTC and TAI time scales using the variables *time* and *time_tai*, respectively. The time of the TVP record in UTC and TAI follow the conventions on time representation described above for *illumination_time* and *illumination_time_tai*. The TVP information for each pixel in the *pixel_cloud* group can be obtained by matching the nearest TVP time with the pixel illumination time. The TVP sampling rate follows the SLC along-track sampling rate.

- *time*: Time in UTC time scale (seconds since January 1, 2000 00:00:00 UTC which is equivalent to January 1, 2000 00:00:32 TAI)
- *time_tai*: Time in TAI time scale (seconds since January 1, 2000 00:00:00 TAI, which is equivalent to December 31, 1999 23:59:28 UTC)

4.1.3.2 Location, Velocity and Attitude

The position, velocity, and attitude of the KaRIn reference frame (KMSF) are given relative to the ITRF in the variables described in this section.

The attitude angles are defined as follows. Let v_{KMSF}, v_{NED}, and v_{ENU} be the same vector represented in KMSF, in the local north-east-down (NED) frame, and in the local east-north-up (ENU) frame, respectively, with the rotation matrices R_{NED}^{KMSF} and R_{ENU}^{NED} giving the transformations between the three vectors representations:

$$v_{KMSF} = R_{NED}^{KMSF} v_{NED}$$
$$v_{NED} = R_{ENU}^{NED} v_{ENU}.$$

These rotation matrices are given by

$$R_{NED}^{KMSF} = \begin{bmatrix} 1 & 0 & 0 \\ 0 & \cos r & \sin r \\ 0 & -\sin r & \cos r \end{bmatrix} \begin{bmatrix} \cos p & 0 & -\sin p \\ 0 & 1 & 0 \\ \sin p & 0 & \cos p \end{bmatrix} \begin{bmatrix} \cos h_p & \sin h_p & 0 \\ -\sin h_p & \cos h_p & 0 \\ 0 & 0 & 1 \end{bmatrix}$$

$$R_{ENU}^{NED} = \begin{bmatrix} 0 & 1 & 0 \\ 1 & 0 & 0 \\ 0 & 0 & -1 \end{bmatrix}$$

where *r* and *p* represent the *roll* and *pitch* variables, and the platform heading h_p is defined as the sum of the *velocity_heading* variable h_v and the *yaw* variable h_y

$$h_p = h_v + h_y$$

with all of these angles defined modulo 360˚.

- *latitude*, *longitude*, *altitude*: Geodetic latitude, longitude, and altitude above the

© 2025 California Institute of Technology. Government sponsorship acknowledged.

reference ellipsoid of the origin of the KMSF frame. The global attributes *ellipsoid_semi_major_axis* and *ellipsoid_flattening* define the reference ellipsoid.

- *roll*, *pitch*, *yaw, velocity_heading*: Attitude of the KMSF frame with respect to the local frame at the location given by *latitude* and *longitude*. The velocity heading is the angle with respect to true north of the nadir track direction such that if the spacecraft were flying due east, the velocity heading would be 90˚. The yaw is the angle of right-handed rotation of the nominal KMSF +*x* axis about the nadir direction. If the KMSF +*x* axis is aligned with the horizontal projection of the Earth-relative spacecraft velocity vector, the yaw will be zero. If the KMSF -*x* axis is aligned with the horizontal projection of the Earth-relative spacecraft velocity vector, the yaw will be 180˚. The heading of the KMSF +*x* axis relative to true north is consequently the sum of the velocity heading and the yaw (modulo 360˚). The pitch is defined such that a positive pitch moves the KMSF axis +*x* up. The roll is defined such that a positive roll moves the +*y* antenna down. Note that when the yaw is near 180˚, the sense of pitch and roll may be counterintuitive to users who are accustomed to airborne platforms since the spacecraft would be flying "tail first."
- *x*, *y*, *z*: Position vector of the KMSF origin in ECEF coordinates.
- *vx*, *vy*, *vz*: Earth-relative velocity vector of the KMSF origin in ECEF coordinates. This velocity vector describes the spacecraft motion in an Earth-fixed (not inertial) frame.

4.1.3.3 Antenna Phase Center Positions

The positions of the phase centers of the two interferometric antennas for the given swath are given at each time point in ECEF coordinates in the following variables:

- *plus_y_antenna_x*, *plus_y_antenna_y*, *plus_y_antenna_z*: Position vector of the +*y* KaRIn antenna phase center in ECEF coordinates.
- *minus_y_antenna_x*, *minus_y_antenna_y*, *minus_y_antenna_z*: Position vector of the –*y* KaRIn antenna phase center in ECEF coordinates.

4.1.3.4 Index in HR Data Collection

The index of the presummed line corresponding to the TVP record relative to the start of the HR data collection captures information about the KaRIn state and allows for decimation in processing to maintain the continuity of sampling across tile boundaries.

- *record_counter*: Index (from 1) relative to the start of the HR datatake of the SLC line corresponding to the TVP record. This counter is used to align data samples across granules.

4.1.3.5 Flags

Flags in the TVP group capture information about the spacecraft and instrument state as described below. The flags should nominally be zero; nonzero values indicate off-nominal conditions. These flags typically give additional information for off-nominal conditions that are reported in the *interferogram_qual*, *classification_qual*, *geolocation_qual*, *sig0_qual,* and *pixc_line_qual* flags.

- *sc_event_flag*: Bit flag whose individual bits indicate spacecraft events that may

© 2025 California Institute of Technology. Government sponsorship acknowledged.

affect the characteristics of the KaRIn data. An off-nominal spacecraft state does not necessarily always imply that the data are not useful, but users should exercise caution in interpreting the data. The bits are defined in rough order of increasing expected measurement degradation from least significant bit to most significant bit. Therefore, if the flag is interpreted as an unsigned, 8 bit integer, then a value of zero (all bits = 0) represents the nominal spacecraft state, nonzero values less than 64 represent "use with caution" (may be degraded, but possibly useful), and values of 64 or greater represent bad measurement quality. The meanings of the flag bits are defined as follows:

  - 1 (Bit 0=1): The measurement may be affected by a yaw-flip maneuver.
  - 2 (Bit 1=1): The measurement may be affected by a gyro calibraton maneuver.
  - 4 (Bit 2=1): The measurement may be affected by an orbit control maneuver.
  - 8 (Bit 3=1): The measurement may be affected by a solar array rotation.
  - 16 (Bit 4=1): The measurement may be affected by an entry of the spacecraft into Earth eclipse.
  - 32 (Bit 5=1): The measurement may be affected by an exit of the spacecraft from Earth eclipse.
  - 64 (Bit 6=1): The measurement is likely bad due to an eclipse event.
  - 128 (Bit 7=1): The measurement is likely bad due to an event other than an eclipse event.

- *tvp_qual*: Flag that indicates the quality of the reconstructed attitude and orbit ephemeris. A value of 0 indicates that the reconstructed attitude and orbit ephemeris are both good. A nonzero value indicates that these data are off-nominal or bad, with the expected degradation of measurement quality roughly increasing with flag value. The value in the tens digit indicates the quality of the reconstructed attitude, and the value in the ones digit represents the quality of the orbit ephemeris for the spacecraft center of mass (but note that the attitude is required to compute the KMSF origin from the center of mass). Non-zero values of *tvp_qual* less than 20 indicate suspect data; values greater than or equal to 20 indicate bad data. The values are as follows:

  - 0: The reconstructed attitude is good and the ephemeris is adjusted on actual tracking data.
  - 4: The reconstructed attitude is good and the ephemeris is estimated during a maneuver.
  - 5: The reconstructed attitude is good and the ephemeris is interpolated over a data gap.
  - 6: The reconstructed attitude is good and the ephemeris is extrapolated over a duration less than 1 day.
  - 7: The reconstructed attitude is good and the ephemeris is extrapolated over a duration between 1 and 2 days.
  - 8: The reconstructed attitude is good and the ephemeris is extrapolated over a duration greater than 2 days.
  - 10: The reconstructed attitude is suspect and the ephemeris is adjusted on actual tracking data.
  - 14: The reconstructed attitude is suspect and the ephemeris is estimated during a maneuver.

© 2025 California Institute of Technology. Government sponsorship acknowledged.

- 15: The reconstructed attitude is suspect and the ephemeris is interpolated over a data gap.
- 16: The reconstructed attitude is suspect and the ephemeris is extrapolated over a duration less than 1 day.
- 17: The reconstructed attitude is suspect and the ephemeris is extrapolated over a duration between 1 and 2 days.
- 18: The reconstructed attitude is suspect and the ephemeris is extrapolated over a duration greater than 2 days.
- 20: The reconstructed attitude is bad and the ephemeris is adjusted on actual tracking data.
- 24: The reconstructed attitude is bad and the ephemeris is estimated during a maneuver.
- 25: The reconstructed attitude is bad and the ephemeris is interpolated over a data gap.
- 26: The reconstructed attitude is bad and the ephemeris is extrapolated over a duration less than 1 day.
- 27: The reconstructed attitude is bad and the ephemeris is extrapolated over a duration between 1 and 2 days.
- 28: The reconstructed attitude is bad and the ephemeris is extrapolated over a duration greater than 2 days.

4.1.4 Noise Group Data

The *noise* group contains estimates of the KaRIn instrument noise for each echo as produced during SLC processing of KaRIn calibration data. The noise samples are not necessarily independent.

- *noise_plus_y*, *noise_minus_y*: Noise powers of the +*y* and –*y* KaRIn antenna channels. The noise power is given in arbitrary linear units that are consistent with the units used to express the signal power (*power_plus_y*, *power_minus_y*, *coherent_power*). The noise power is related to the noise-equivalent sigma0 (NESZ) through the X factor (*x_factor_plus_y*, *x_factor_minus_y*).

© 2025 California Institute of Technology. Government sponsorship acknowledged.

5 Detailed Product Description

The L2_HR_PIXC adopts a NetCDF-4 file format and conventions. This is a self-documenting format that contains metadata as global attributes, dimensions, variables, and attributes for variables. Each file contains multiple NetCDF groups of data as described above. Global attributes are defined both outside and potentially inside the groups. The global attributes that are defined outside of the groups (i.e., the root netcdf group) apply to all groups in the file, while global attributes that occur within each data group apply to only all of the data within that single group. Variable attributes only apply to the associated variable. The NetCDF command "ncdump –h product.nc" can be used to view the header of the product, which describes the content of the product.

5.1 NetCDF Variables

Variables are used to store the various measurements. Each variable is assigned a name and a particular data type. Variables can be scalar values (i.e. 0 dimension), or can have one or more of the dimensions. Each variable then has attributes that provide additional information about the variable. Table 4 below identifies the data types used in the L2_HR_PIXC product, and Table 5 identifies the attributes that may be assigned to each variable.

Table 4. Variable data types in NetCDF products.

Data Type	Description
char	characters (ASCII)
byte	8-bit signed integer
unsigned byte	8-bit unsigned integer
short	16-bit signed integer
unsigned short	16-bit unsigned integer
int	32-bit signed integer
unsigned int	32-bit unsigned integer
long	64-bit signed integer
unsigned long	64-bit unsigned integer
float	IEEE single precision floating point (32 bits)
double	IEEE double precision floating point (64 bits)

Table 5. Common variable attributes in NetCDF files.

Attribute	Description
_FillValue	The value used to represent missing or undefined data. (Before applying add_offset and scale_factor).
add_offset	If present this value should be added to each data element after it is read. If both scale_factor and add_offset attributes are present, the data are first scaled before the offset is added.
calendar	Reference time calendar
comment	Miscellaneous information about the data or the methods to generate it.
coordinates	Coordinate variables associated with the variable
flag_meanings	Used in conjunction with flag_values or flag_masks. Describes the meanings of each of the elements of flag_values or flag_masks.
flag_values	Used in conjunction with flag_meanings. Possible values of the flag variable.

© 2025 California Institute of Technology. Government sponsorship acknowledged.

flag_masks	Used in conjunction with flag_meanings. Describes a number of independent Boolean conditions using bit field notation by setting unique bits in each flag_masks value. A flagged condition is identified by performing a bitwise AND of the variable value and each flag_masks value; a non-zero result indicates a true condition. Thus, any or all of the flagged conditions may be true, depending on the variable bit settings.
institution	Institution which generates the source data for the variable, if applicable.
leap_second	UTC time at which a leap second occurs within the time span of data within the file.
long_name	A descriptive variable name that indicates its content.
quality_flag	Names of variable quality flag(s) that are associated with this variable to indicate its quality.
scale_factor	If present, the data are to be multiplied by the value after they are read. If both scale_factor and add_offset attributes are present, the data are first scaled before the offset is added.
source	Data source (model, author, or instrument)
standard_name	A standard variable name that indicates its content.
tai_utc_difference	Difference between TAI and UTC reference time.
units	Unit of data after applying offset (add_offset) and scale_factor.
valid_max	Maximum theoretical value of variable before applying scale_factor and add_offset (not necessarily the same as maximum value of actual data)
valid_min	Minimum theoretical value of variable before applying scale_factor and add_offset (not necessarily the same as minimum value of actual data)

5.2 Level 2 KaRIn HR Pixel Cloud File

5.2.1 Global Attributes

Global attributes for the L2_HR_PIXC product are provided in Table 6 below.

Table 6. Global attributes for all data groups in the L2_HR_PIXC product file.

Attribute	Format	Description
Conventions	string	NetCDF-4 conventions adopted in this group. This attribute should be set to CF-1.7 to indicate that the group is compliant with the Climate and Forecast NetCDF conventions.
title	string	Level 2 KaRIn High Rate Water Mask Pixel Cloud Data Product
institution	string	Name of producing agency.
source	string	The method of production of the original data. If it was model-generated, source should name the model and its version, as specifically as could be useful. If it is observational, source should characterize it (e.g., 'Ka-band radar interferometer').
history	string	UTC time when file generated. Format is: 'YYYY-MM-DDThh:mm:ssZ : Creation'
platform	string	SWOT
references	string	Published or web-based references that describe the data or methods used to product it. Provides version number of software generating product.
reference_document	string	Name and version of Product Description Document to use as reference for product.
contact	string	Contact information for producer of product. (e.g., 'ops@jpl.nasa.gov').

© 2025 California Institute of Technology. Government sponsorship acknowledged.

cycle_number	short	Cycle number of the product granule.
pass_number	short	Pass number of the product granule.
tile_number	short	Tile number in the pass of the product granule.
swath_side	string	'L' or 'R' to indicate left and right swath, respectively.
tile_name	string	Tile name using format PPP_TTTS, where PPP is a 3 digit pass number with leading zeros, TTT is a 3 digit tile number within the pass, and S is a character 'L' or 'R' for the left and right swath, respectively.
short_name	string	L2_HR_PIXC
crid	string	Composite release identifier (CRID) of the data system used to generate this file
product_version	string	Version identifier of this data file
pge_name	string	Name of the product generation executable (PGE) that created this file
pge_version	string	Version identifier of the product generation executable (PGE) that created this file
time_granule_start	string	Nominal starting UTC time of product granule. Format is: YYYY-MM-DDThh:mm:ss.ssssssZ
time_granule_end	string	Nominal ending UTC time of product granule. Format is: YYYY-MM-DDThh:mm:ss.ssssssZ
time_coverage_start	string	UTC time of first measurement. Format is: YYYY-MM-DDThh:mm:ss.ssssssZ
time_coverage_end	string	UTC time of last measurement. Format is: YYYY-MM-DDThh:mm:ss.ssssssZ
geospatial_lon_min	double	Westernmost longitude (deg) of granule bounding box
geospatial_lon_max	double	Easternmost longitude (deg) of granule bounding box
geospatial_lat_min	double	Southernmost latitude (deg) of granule bounding box
geospatial_lat_max	double	Northernmost latitude (deg) of granule bounding box
inner_first_longitude	double	Nominal swath corner longitude for the first range line and inner part of the swath (degrees_east)
inner_first_latitude	double	Nominal swath corner latitude for the first range line and inner part of the swath (degrees_north)
inner_last_longitude	double	Nominal swath corner longitude for the last range line and inner part of the swath (degrees_east)
inner_last_latitude	double	Nominal swath corner latitude for the last range line and inner part of the swath (degrees_north)
outer_first_longitude	double	Nominal swath corner longitude for the first range line and outer part of the swath (degrees_east)
outer_first_latitude	double	Nominal swath corner latitude for the first range line and outer part of the swath (degrees_north)
outer_last_longitude	double	Nominal swath corner longitude for the last range line and outer part of the swath (degrees_east)
outer_last_latitude	double	Nominal swath corner latitude for the last range line and outer part of the swath (degrees_north)
wavelength	double	Wavelength (m) of the transmitted signal, which is determined based on the transmitter center frequency of the transmit chirp.
near_range	double	The slant range (m) for the first image pixel.
nominal_slant_range_spacing	double	The range spacing (m) corresponding to the 200 MHz sampling frequency
polarization	string	Flag indicating whether the tile was observed with a horizontal (H) or vertical (V) radar signal polarization.
transmit_antenna	string	Flag indicating which of the KaRIn antennas (plus_y or minus_y) is transmitting.

© 2025 California Institute of Technology. Government sponsorship acknowledged.

processing_beamwidth	double	Beamwidth (deg) used to integrate the range compressed data in azimuth compression. The 3 dB nominal azimuth antenna pattern beamwidth is about 0.1 degrees. After on-board presum with a presum factor of 2.125, the effective beamwidth is reduced to about 0.05 degrees.
slc_along_track_resolution	double	Along-track or azimuth resolution (m) corresponding to the processing beamwidth for the SLC data. The resolution is approximately the width between half-power points of the main lobe of the image point target response assuming that targets do not decorrelate over the focusing aperture time (which is not the case for water because of the short coherence time).
slc_range_resolution	double	Range resolution (m) for the SLC data. The resolution is approximately the half-power width of the range point target response.
slc_first_line_index_in_tvp	int	The TVP index (from 0) corresponding to the first SLC image line in the overlapped tile.
slc_last_line_index_in_tvp	int	The TVP index (from 0) corresponding to the last SLC image line in the overlapped tile.
kmsf_to_dop_roll	double	The KMSF to Doppler frame roll bias angle in degrees. A positive sign moves the Doppler frame +y axis down relative to KMSF. This parameter is part of a common rotation used for both antennas so that the SLC images are processed to the same Doppler centroid.
kmsf_to_dop_pitch	double	The KMSF to Doppler frame pitch angle in degrees. A positive sign moves the Doppler frame +x axis up relative to KMSF. This parameter is part of a common rotation used for both antennas so that the SLC images are processed to the same Doppler centroid.
kmsf_to_dop_yaw	double	The KMSF to Doppler frame yaw angle in degrees. A positive sign moves the Doppler frame +x axis right relative to KMSF. This parameter is part of a common rotation used for both antennas so that the SLC images are processed to the same Doppler centroid.
xref_l1b_hr_slc_file	string	Name of input Level 1B high rate single look complex file.
xref_int_lr_xover_cal_file	string	Name of input low rate crossover calibration file.
xref_statickarincal_files	string	Names of input static KaRIn calibration files.
xref_param_l2_hr_pixc_file	string	Name of input Level 2 high rate pixel cloud processor configuration parameters file.
xref_refdem_file	string	Name of input reference digital elevation model file.
xref_watermask_files	string	Names of input water mask files.
xref_reforbittrack_files	string	Names of input reference orbit track files.
xref_meteorological_orography_files	string	Names of input meteorological model orography files.
xref_meteorological_specific_humidity_files	string	Names of input meteorological model specific humidity profile files.
xref_meteorological_temperature_profile_files	string	Names of input meteorological model temperature profile files.
xref_meteorological_specific_cloud_liquid_water_files	string	Names of input meteorological model specific cloud liquid water profile files.
xref_meteorological_surface_pressure_files	string	Names of input meteorological model uncorrected pressure files.
xref_gim_files	string	Names of input global ionosphere map (GIM) files.
xref_pole_location_file	string	Name of input pole location file.
xref_geco_database_version	string	Version number of geophysical and environmental corrections static database. Provides models for surface classification, geoid, load tides, pole tide, monthly and diurnal atmospheric pressure climatology.

© 2025 California Institute of Technology. Government sponsorship acknowledged.

ellipsoid_semi_major_axis	double	Semi-major axis of reference ellipsoid in meters.
ellipsoid_flattening	double	Flattening of reference ellipsoid

5.2.2 Group Names, Attributes, and Dimensions

As described in Table 2, the L2_HR_PIXC product file contains three NetCDF data groups called the *pixel_cloud*, *tvp*, and *noise* groups.

Each group has a 'description' attribute that elaborates on what the data in the group represents. The *pixel_cloud* data group has some extra group attributes. The attributes of the pixel cloud, tvp, and noise groups are summarized in Tables 8-10.

Each NetCDF group uses the dimensions attributes to identify the physical dimensions of variables within that single group. The L2_HR_PIXC product uses different combinations of the dimensions shown in Table 10 for the variables within each group.

Table 7. Attributes of the *pixel_cloud* group of the L2_HR_PIXC product.

Attribute	Format	Description
description	string	cloud of geolocated interferogram pixels
interferogram_size_azimuth	int	number of azimuth rows of interferogram image
interferogram_size_range	int	number of range-bin columns of interferogram image
looks_to_efflooks	double	ratio of the number of real looks to the effective number of independent looks
num_azimuth_looks	double	number of real azimuth looks commanded in rare multilooking
azimuth_offset	int	offset number of slc lines used in rare multilooking to keep overlapping portion of consecutive tiles to be consistent for the 2D rare interferogram images before pruning

Table 8. Attributes of the *tvp* group of the L2_HR_PIXC product.

Attribute	Format	Description
description	string	Time varying parameters group including spacecraft attitude, position, velocity, and antenna position information
mean_pitch_correction	double	Mean effective pitch correction in degrees over the granule as derived from the Doppler estimate of the KaRIn data, if applicable. This value is 0 if the processed Doppler is based only on attitude information.

Table 9. Attributes of the *noise* group of the L2_HR_PIXC product.

Attribute	Format	Description
description	string	Measured noise power for each receive echo of the plus_y and minus_y SLC channels

Table 10. Dimensions of variables within each NetCDF data group.

Name	Description
complex_depth	complex_depth is the name of the dimension that stores the real and imaginary components of complex values in arrays holding complex data. Therefore, the number of elements in this dimension is always 2.
num_tvps	The number of TVP records inherited from the raw data from which the SLC image is processed.
points	The number of pixels in the pixel cloud data.
num_lines	The number of along-track lines of the Noise data (and the SLC and X factor image data in the SLC

© 2025 California Institute of Technology. Government sponsorship acknowledged.

	product).
num_pixc_lines	The number of along-track lines of the pixel-cloud slant-plane data (similar to num_lines, but at the rare interferogram posting).

5.2.3 Detailed NetCDF Format Description

This section provides a detailed listing of each of the variables within each of the groups of the L2_HR_PIXC product and their associated variable attributes.

Table 11. Variables of the *pixel_cloud* group of the L2_HR_PIXC product.

Group pixel_cloud Variables		
int azimuth_index(points)		
	_FillValue	2147483647
	long_name	rare interferogram azimuth index
	units	1
	valid_min	0
	valid_max	999999
	coordinates	longitude latitude
	comment	Rare interferogram azimuth index (indexed from 0).
int range_index(points)		
	_FillValue	2147483647
	long_name	rare interferogram range index
	units	1
	valid_min	0
	valid_max	999999
	coordinates	longitude latitude
	comment	Rare interferogram range index (indexed from 0).
float interferogram(points, complex_depth)		
	_FillValue	9.96921e+36
	long_name	rare interferogram
	units	1
	quality_flag	interferogram_qual
	valid_min	-1e+20
	valid_max	1e+20
	coordinates	longitude latitude
	comment	Complex unflattened rare interferogram.
float power_plus_y(points)		
	_FillValue	9.96921e+36
	long_name	power for plus_y channel
	units	1
	quality_flag	interferogram_qual
	valid_min	0
	valid_max	1e+20
	coordinates	longitude latitude
	comment	Power for the plus_y channel (arbitrary units that give sigma0 when noise subtracted and normalized by the X factor).
float power_minus_y(points)		
	_FillValue	9.96921e+36
	long_name	power for minus_y channel
	units	1
	quality_flag	interferogram_qual

© 2025 California Institute of Technology. Government sponsorship acknowledged.

	valid_min	0
	valid_max	1e+20
	coordinates	longitude latitude
	comment	Power for the minus_y channel (arbitrary units that give sigma0 when noise subtracted and normalized by the X factor).
float coherent_power(points)		
	_FillValue	9.96921e+36
	long_name	coherent power combination of minus_y and plus_y channels
	units	1
	quality_flag	interferogram_qual
	valid_min	0
	valid_max	1e+20
	coordinates	longitude latitude
	comment	Power computed by combining the plus_y and minus_y channels coherently by co-aligning the phases (arbitrary units that give sigma0 when noise subtracted and normalized by the X factor).
float x_factor_plus_y(points)		
	_FillValue	9.96921e+36
	long_name	X factor for plus_y channel power
	units	1
	valid_min	0
	valid_max	1e+20
	coordinates	longitude latitude
	comment	X factor for the plus_y channel power in linear units (arbitrary units to normalize noise-subtracted power to sigma0).
float x_factor_minus_y(points)		
	_FillValue	9.96921e+36
	long_name	X factor for minus_y channel power
	units	1
	valid_min	0
	valid_max	1e+20
	coordinates	longitude latitude
	comment	X factor for the minus_y channel power in linear units (arbitrary units to normalize noise-subtracted power to sigma0).
float water_frac(points)		
	_FillValue	9.96921e+36
	long_name	water fraction
	units	1
	quality_flag	classification_qual
	valid_min	-1000
	valid_max	10000
	coordinates	longitude latitude
	comment	Noisy estimate of the fraction of the pixel that is water.
float water_frac_uncert(points)		
	_FillValue	9.96921e+36
	long_name	water fraction uncertainty
	units	1
	valid_min	0
	valid_max	999999
	coordinates	longitude latitude
	comment	Uncertainty estimate of the water fraction estimate (width of noisy water frac estimate distribution).
unsigned byte classification(points)		

© 2025 California Institute of Technology. Government sponsorship acknowledged.

	_FillValue	255
	long_name	classification
	quality_flag	classification_qual
	flag_meanings	land land_near_water water_near_land open_water dark_water low_coh_water_near_land open_low_coh_water
	flag_values	1 2 3 4 5 6 7
	valid_min	1
	valid_max	7
	coordinates	longitude latitude
	comment	Flags indicating water detection results.
float false_detection_rate(points)		
	_FillValue	9.96921e+36
	long_name	false detection rate
	units	1
	quality_flag	classification_qual
	valid_min	0
	valid_max	1
	coordinates	longitude latitude
	comment	Probability of falsely detecting water when there is none.
float missed_detection_rate(points)		
	_FillValue	9.96921e+36
	long_name	missed detection rate
	units	1
	quality_flag	classification_qual
	valid_min	0
	valid_max	1
	coordinates	longitude latitude
	comment	Probability of falsely detecting no water when there is water.
float prior_water_prob(points)		
	_FillValue	9.96921e+36
	long_name	prior water probability
	units	1
	valid_min	0
	valid_max	1
	coordinates	longitude latitude
	comment	Prior probability of water occurring.
float prior_water_change(points)		
	_FillValue	9.96921e+36
	long_name	prior water change
	units	1
	valid_min	-1
	valid_max	1
	coordinates	longitude latitude
	comment	Normalized value that qualitatively indicates the long-term change in the probability of water based on prior data (positive values indicate increasing probability).
unsigned byte bright_land_flag(points)		
	_FillValue	255
	long_name	bright land flag
	standard_name	status_flag
	flag_meanings	not_bright_land bright_land bright_land_or_water
	flag_values	0 1 2
	valid_min	0
	valid_max	2

© 2025 California Institute of Technology. Government sponsorship acknowledged.

	coordinates	longitude latitude
	comment	Flag indicating areas that are not typically water but are expected to be bright (e.g., urban areas, ice). Flag value 2 indicates cases where prior data indicate land, but where prior_water_prob indicates possible water.
float layover_impact(points)		
	_FillValue	9.96921e+36
	long_name	layover impact
	units	m
	valid_min	-999999
	valid_max	999999
	coordinates	longitude latitude
	comment	Estimate of the height error caused by layover, which may not be reliable on a pixel by pixel basis, but may be useful to augment aggregated height uncertainties.
float eff_num_rare_looks(points)		
	_FillValue	9.96921e+36
	long_name	effective number of rare looks
	units	1
	valid_min	0
	valid_max	999999
	coordinates	longitude latitude
	comment	Effective number of independent looks taken to form the rare interferogram.
double latitude(points)		
	_FillValue	9.969209968386869e+36
	long_name	latitude (positive N, negative S)
	standard_name	latitude
	units	degrees_north
	quality_flag	geolocation_qual
	valid_min	-80
	valid_max	80
	comment	Geodetic latitude [-80,80] (degrees north of equator) of the pixel.
double longitude(points)		
	_FillValue	9.969209968386869e+36
	long_name	longitude (degrees East)
	standard_name	longitude
	units	degrees_east
	quality_flag	geolocation_qual
	valid_min	-180
	valid_max	180
	comment	Longitude [-180,180) (east of the Greenwich meridian) of the pixel.
float height(points)		
	_FillValue	9.96921e+36
	long_name	height above reference ellipsoid
	units	m
	quality_flag	geolocation_qual
	valid_min	-1500
	valid_max	15000
	coordinates	longitude latitude
	comment	Height of the pixel above the reference ellipsoid.
float cross_track(points)		
	_FillValue	9.96921e+36
	long_name	approximate cross-track location
	units	m
	quality_flag	geolocation_qual

© 2025 California Institute of Technology. Government sponsorship acknowledged.

	valid_min	-75000
	valid_max	75000
	coordinates	longitude latitude
	comment	Approximate cross-track location of the pixel.
float pixel_area(points)		
	_FillValue	9.96921e+36
	long_name	pixel area
	units	m^2
	quality_flag	geolocation_qual
	valid_min	0
	valid_max	999999
	coordinates	longitude latitude
	comment	Pixel area.
float inc(points)		
	_FillValue	9.96921e+36
	long_name	incidence angle
	units	degrees
	quality_flag	geolocation_qual
	valid_min	0
	valid_max	999999
	coordinates	longitude latitude
	comment	Incidence angle.
float phase_noise_std(points)		
	_FillValue	9.96921e+36
	long_name	phase noise standard deviation
	units	radians
	valid_min	-999999
	valid_max	999999
	coordinates	longitude latitude
	comment	Estimate of the phase noise standard deviation.
float dlatitude_dphase(points)		
	_FillValue	9.96921e+36
	long_name	sensitivity of latitude estimate to interferogram phase
	units	degrees/radian
	quality_flag	geolocation_qual
	valid_min	-999999
	valid_max	999999
	coordinates	longitude latitude
	comment	Sensitivity of the latitude estimate to the interferogram phase.
float dlongitude_dphase(points)		
	_FillValue	9.96921e+36
	long_name	sensitivity of longitude estimate to interferogram phase
	units	degrees/radian
	quality_flag	geolocation_qual
	valid_min	-999999
	valid_max	999999
	coordinates	longitude latitude
	comment	Sensitivity of the longitude estimate to the interferogram phase.
float dheight_dphase(points)		
	_FillValue	9.96921e+36
	long_name	sensitivity of height estimate to interferogram phase
	units	m/radian
	quality_flag	geolocation_qual

© 2025 California Institute of Technology. Government sponsorship acknowledged.

	valid_min	-999999
	valid_max	999999
	coordinates	longitude latitude
	comment	Sensitivity of the height estimate to the interferogram phase.
float dheight_droll(points)		
	_FillValue	9.96921e+36
	long_name	sensitivity of height estimate to spacecraft roll
	units	m/degrees
	quality_flag	geolocation_qual
	valid_min	-999999
	valid_max	999999
	coordinates	longitude latitude
	comment	Sensitivity of the height estimate to the spacecraft roll.
float dheight_dbaseline(points)		
	_FillValue	9.96921e+36
	long_name	sensitivity of height estimate to interferometric baseline
	units	m/m
	quality_flag	geolocation_qual
	valid_min	-999999
	valid_max	999999
	coordinates	longitude latitude
	comment	Sensitivity of the height estimate to the interferometric baseline.
float dheight_drange(points)		
	_FillValue	9.96921e+36
	long_name	sensitivity of height estimate to range (delay)
	units	m/m
	quality_flag	geolocation_qual
	valid_min	-999999
	valid_max	999999
	coordinates	longitude latitude
	comment	Sensitivity of the height estimate to the range (delay).
float darea_dheight(points)		
	_FillValue	9.96921e+36
	long_name	sensitivity of pixel area to reference height
	units	m^2/m
	quality_flag	geolocation_qual
	valid_min	-999999
	valid_max	999999
	coordinates	longitude latitude
	comment	Sensitivity of the pixel area to the reference height.
double illumination_time(points)		
	_FillValue	9.969209968386869e+36
	long_name	time of illumination of each pixel (UTC)
	standard_name	time
	calendar	gregorian
	tai_utc_difference	[Value of TAI-UTC at time of first record]
	leap_second	YYYY-MM-DDThh:mm:ssZ
	units	seconds since 2000-01-01 00:00:00.000
	comment	Time of measurement in seconds in the UTC time scale since 1 Jan 2000 00:00:00 UTC. [tai_utc_difference] is the difference between TAI and UTC reference time (seconds) for the first measurement of the data set. If a leap second occurs within the data set, the attribute leap_second is set to the UTC time at which the leap second occurs.

© 2025 California Institute of Technology. Government sponsorship acknowledged.

double illumination_time_tai(points)		
	_FillValue	9.969209968386869e+36
	long_name	time of illumination of each pixel (TAI)
	standard_name	time
	calendar	gregorian
	units	seconds since 2000-01-01 00:00:00.000
	comment	Time of measurement in seconds in the TAI time scale since 1 Jan 2000 00:00:00 TAI. This time scale contains no leap seconds. The difference (in seconds) with time in UTC is given by the attribute [illumination_time:tai_utc_difference].
float eff_num_medium_looks(points)		
	_FillValue	9.96921e+36
	long_name	effective number of medium looks
	units	1
	valid_min	0
	valid_max	999999
	coordinates	longitude latitude
	comment	Effective number of independent looks taken in forming the medium interferogram (after adaptive averaging).
float sig0(points)		
	_FillValue	9.96921e+36
	long_name	sigma0
	units	1
	quality_flag	sig0_qual
	valid_min	-999999
	valid_max	999999
	coordinates	longitude latitude
	comment	Normalized radar cross section (sigma0) in real, linear units (not decibels). The value may be negative due to noise subtraction.
float sig0_uncert(points)		
	_FillValue	9.96921e+36
	long_name	sigma0 uncertainty
	units	1
	valid_min	-999999
	valid_max	999999
	coordinates	longitude latitude
	comment	1-sigma uncertainty in the sig0 measurement. The value is given as an additive (not multiplicative) linear term (not a term in decibels).
int phase_unwrapping_region(points)		
	_FillValue	2147483647
	long_name	phase unwrapping region index
	units	1
	valid_min	-1
	valid_max	99999999
	coordinates	longitude latitude
	comment	Phase unwrapping region index.
float ambiguity_cost1(points)		
	_FillValue	9.96921e+36
	long_name	phase ambiguity minimum cost
	units	1
	valid_min	-999999
	valid_max	999999
	coordinates	longitude latitude
	comment	Phase ambiguity minimum cost.

© 2025 California Institute of Technology. Government sponsorship acknowledged.

float ambiguity_cost2(points)		
	_FillValue	9.96921e+36
	long_name	phase ambiguity 2nd minimum cost
	units	1
	valid_min	-999999
	valid_max	999999
	coordinates	longitude latitude
	comment	Phase ambiguity 2nd minimum cost.
float instrument_range_cor(points)		
	_FillValue	9.96921e+36
	long_name	instrument range correction
	units	m
	valid_min	-999999
	valid_max	999999
	coordinates	longitude latitude
	comment	Term that incorporates all calibration corrections applied to range before geolocation.
float instrument_phase_cor(points)		
	_FillValue	9.96921e+36
	long_name	instrument phase correction
	units	radians
	valid_min	-999999
	valid_max	999999
	coordinates	longitude latitude
	comment	Term that incorporates all calibration corrections applied to phase before geolocation.
float instrument_baseline_cor(points)		
	_FillValue	9.96921e+36
	long_name	instrument baseline correction
	units	m
	valid_min	-999999
	valid_max	999999
	coordinates	longitude latitude
	comment	Term that incorporates all calibration corrections applied to baseline before geolocation.
float sig0_cor_atmos_model(points)		
	_FillValue	9.96921e+36
	long_name	two-way atmospheric correction to sigma0 from model
	source	European Centre for Medium-Range Weather Forecasts
	institution	ECMWF
	units	1
	valid_min	1
	valid_max	10
	coordinates	longitude latitude
	comment	Atmospheric correction to sigma0 from weather model data as a linear power multiplier (not decibels). sig0_cor_atmos_model is already applied in computing sig0 and x_factor_plus_y and x_factor_minus_y.
float height_cor_xover(points)		
	_FillValue	9.96921e+36
	long_name	height correction from KaRIn crossovers
	units	m
	valid_min	-10
	valid_max	10
	coordinates	longitude latitude

© 2025 California Institute of Technology. Government sponsorship acknowledged.

	comment	Height correction from KaRIn crossover calibration. The correction is applied before geolocation but reported as an equivalent height correction.
float model_dry_tropo_cor(points)		
	_FillValue	9.96921e+36
	long_name	dry troposphere vertical correction
	source	European Centre for Medium-Range Weather Forecasts
	institution	ECMWF
	units	m
	valid_min	-3
	valid_max	-1.5
	coordinates	longitude latitude
	comment	Equivalent vertical correction due to dry troposphere delay. The reported pixel height, latitude and longitude are computed after adding negative media corrections to uncorrected range along slant-range paths, accounting for the differential delay between the two KaRIn antennas. The equivalent vertical correction is computed by applying obliquity factors to the slant-path correction. Adding the reported correction to the reported pixel height results in the uncorrected pixel height.
float model_wet_tropo_cor(points)		
	_FillValue	9.96921e+36
	long_name	wet troposphere vertical correction
	source	European Centre for Medium-Range Weather Forecasts
	institution	ECMWF
	units	m
	valid_min	-1
	valid_max	0
	coordinates	longitude latitude
	comment	Equivalent vertical correction due to wet troposphere delay. The reported pixel height, latitude and longitude are computed after adding negative media corrections to uncorrected range along slant-range paths, accounting for the differential delay between the two KaRIn antennas. The equivalent vertical correction is computed by applying obliquity factors to the slant-path correction. Adding the reported correction to the reported pixel height results in the uncorrected pixel height.
float iono_cor_gim_ka(points)		
	_FillValue	9.96921e+36
	long_name	ionosphere vertical correction
	source	Global Ionosphere Maps
	institution	JPL
	units	m
	valid_min	-0.5
	valid_max	0
	coordinates	longitude latitude
	comment	Equivalent vertical correction due to ionosphere delay. The reported pixel height, latitude and longitude are computed after adding negative media corrections to uncorrected range along slant-range paths, accounting for the differential delay between the two KaRIn antennas. The equivalent vertical correction is computed by applying obliquity factors to the slant-path correction. Adding the reported correction to the reported pixel height results in the uncorrected pixel height.
float geoid(points)		
	_FillValue	9.96921e+36
	long_name	geoid height
	standard_name	geoid_height_above_reference_ellipsoid
	source	EGM2008 (Pavlis et al., 2012)
	units	m
	valid_min	-150

© 2025 California Institute of Technology. Government sponsorship acknowledged.

	valid_max	150
	coordinates	longitude latitude
	comment	Geoid height above the reference ellipsoid with a correction to refer the value to the mean tide system, i.e. includes the permanent tide (zero frequency). This value is reported for reference but is not applied to the reported height.
float solid_earth_tide(points)		
	_FillValue	9.96921e+36
	long_name	solid Earth tide height
	source	Cartwright and Taylor (1971) and Cartwright and Edden (1973)
	units	m
	valid_min	-1
	valid_max	1
	coordinates	longitude latitude
	comment	Solid-Earth (body) tide height. The zero-frequency permanent tide component is not included. This value is reported for reference but is not applied to the reported height.
float load_tide_fes(points)		
	_FillValue	9.96921e+36
	long_name	geocentric load tide height (FES)
	source	FES2022b
	institution	LEGOS/CNES
	units	m
	valid_min	-0.2
	valid_max	0.2
	coordinates	longitude latitude
	comment	Geocentric load tide height. The effect of the ocean tide loading of the Earth's crust. This value is reported for reference but is not applied to the reported height.
float load_tide_got(points)		
	_FillValue	9.96921e+36
	long_name	geocentric load tide height (GOT)
	source	GOT4.10c (Ray, 2013)
	institution	GSFC
	units	m
	valid_min	-0.2
	valid_max	0.2
	coordinates	longitude latitude
	comment	Geocentric load tide height. The effect of the ocean tide loading of the Earth's crust. This value is reported for reference but is not applied to the reported height.
float pole_tide(points)		
	_FillValue	9.96921e+36
	long_name	geocentric pole tide height
	source	Wahr (1985) and Desai et al. (2015)
	units	m
	valid_min	-0.2
	valid_max	0.2
	coordinates	longitude latitude
	comment	Geocentric pole tide height. The total of the contribution from the solid-Earth (body) pole tide height and the load pole tide height (i.e., the effect of the ocean pole tide loading of the Earth's crust). This value is reported for reference but is not applied to the reported height.
unsigned byte ancillary_surface_classification_flag(points)		
	_FillValue	255
	long_name	surface classification
	standard_name	status_flag

© 2025 California Institute of Technology. Government sponsorship acknowledged.

	source	MODIS/GlobCover
	institution	European Space Agency
	flag_meanings	open_ocean land continental_water aquatic_vegetation continental_ice_snow floating_ice salted_basin
	flag_values	0 1 2 3 4 5 6
	valid_min	0
	valid_max	6
	coordinates	longitude latitude
	comment	7-state surface type classification computed from a mask built with MODIS and GlobCover data.
unsigned int interferogram_qual(points)		
	_FillValue	4294967295
	standard_name	status_flag
	flag_meanings	suspect_karin_telem rare_power_suspect rare_phase_suspect tvp_suspect sc_event_suspect small_karin_gap in_air_pixel_degraded specular_ringing_degraded rare_power_bad rare_phase_bad tvp_bad sc_event_bad large_karin_gap
	flag_masks	1024 2048 4096 8192 16384 32768 262144 524288 134217728 268435456 536870912 1073741824 2147483648
	valid_min	0
	valid_max	4161600512
	coordinates	longitude latitude
	comment	Quality flag for the interferogram quantities in the pixel cloud data
unsigned int classification_qual(points)		
	_FillValue	4294967295
	standard_name	status_flag
	flag_meanings	no_coherent_gain power_close_to_noise_floor detected_water_but_no_prior_water detected_water_but_bright_land water_false_detection_rate_suspect suspect_karin_telem coherent_power_suspect tvp_suspect sc_event_suspect small_karin_gap in_air_pixel_degraded specular_ringing_degraded coherent_power_bad tvp_bad sc_event_bad large_karin_gap
	flag_masks	1 2 4 8 16 1024 2048 8192 16384 32768 262144 524288 134217728 536870912 1073741824 2147483648
	valid_min	0
	valid_max	3893160991
	coordinates	longitude latitude
	comment	Quality flag for the classification quantities in the pixel cloud data
unsigned int geolocation_qual(points)		
	_FillValue	4294967295
	standard_name	status_flag
	flag_meanings	layover_significant phase_noise_suspect phase_unwrapping_suspect model_dry_tropo_cor_suspect model_wet_tropo_cor_suspect iono_cor_gim_ka_suspect xovercal_suspect suspect_karin_telem medium_phase_suspect tvp_suspect sc_event_suspect small_karin_gap specular_ringing_degraded model_dry_tropo_cor_missing model_wet_tropo_cor_missing iono_cor_gim_ka_missing xovercal_missing geolocation_is_from_refloc no_geolocation_bad medium_phase_bad tvp_bad sc_event_bad large_karin_gap
	flag_masks	1 2 4 8 16 32 64 1024 4096 8192 16384 32768 524288 1048576 2097152 4194304 8388608 16777216 134217728 268435456 536870912 1073741824 2147483648
	valid_min	0
	valid_max	4193842303
	coordinates	longitude latitude
	comment	Quality flag for the geolocation quantities in the pixel cloud data
unsigned int sig0_qual(points)		

© 2025 California Institute of Technology. Government sponsorship acknowledged.

	_FillValue	4294967295
	standard_name	status_flag
	flag_meanings	sig0_uncert_suspect sig0_cor_atmos_suspect noise_power_suspect xfactor_suspect suspect_karin_telem rare_power_suspect tvp_suspect sc_event_suspect small_karin_gap in_air_pixel_degraded specular_ringing_degraded sig0_cor_atmos_missing noise_power_bad xfactor_bad rare_power_bad tvp_bad sc_event_bad large_karin_gap
	flag_masks	1 2 4 8 1024 2048 8192 16384 32768 262144 524288 1048576 33554432 67108864 134217728 536870912 1073741824 2147483648
	valid_min	0
	valid_max	3994872847
	coordinates	longitude latitude
	comment	Quality flag for sig0
unsigned int pixc_line_qual(num_pixc_lines)		
	_FillValue	4294967295
	standard_name	status_flag
	flag_meanings	not_in_tile suspect_karin_telem tvp_suspect sc_event_suspect small_karin_gap tvp_bad sc_event_bad large_karin_gap
	flag_masks	1 1024 8192 16384 32768 536870912 1073741824 2147483648
	valid_min	0
	valid_max	3758154753
	comment	Quality flag for pixel cloud data per rare-posted interferogram line (similar to slc_qual in the L1B_HR_SLC product)
float pixc_line_to_tvp(num_pixc_lines)		
	_FillValue	9.96921e+36
	long_name	pixel cloud rare line to tvp index
	units	1
	valid_min	0
	valid_max	999999
	comment	Pixel cloud rare radar grid line index to tvp index mapping
int data_window_first_valid(num_pixc_lines)		
	_FillValue	2147483647
	long_name	pixel cloud data window starting index
	units	1
	valid_min	0
	valid_max	999999
	comment	Pixel cloud data window starting index of first valid pixel in the range direction
int data_window_last_valid(num_pixc_lines)		
	_FillValue	2147483647
	long_name	pixel cloud data window ending index
	units	1
	valid_min	0
	valid_max	999999
	comment	Pixel cloud data window ending index of last valid pixel in the range direction
float data_window_first_cross_track(num_pixc_lines)		
	_FillValue	9.96921e+36
	long_name	pixel cloud data window starting cross-track distance
	units	m
	valid_min	-75000
	valid_max	75000
	comment	Pixel cloud data window starting cross-track distance in meters of first valid pixel in the range direction
float data_window_last_cross_track(num_pixc_lines)		

© 2025 California Institute of Technology. Government sponsorship acknowledged.

	_FillValue	9.96921e+36
	long_name	pixel cloud data window ending cross-track distance
	units	m
	valid_min	-75000
	valid_max	75000
	comment	Pixel cloud data window ending cross-track distance in meters of last valid pixel in the range direction

Table 12. Variables of the tvp group of the L2_HR_PIXC product.

Group tvp Variables		
double time(num_tvps)		
	_FillValue	9.969209968386869e+36
	long_name	time in UTC
	standard_name	time
	calendar	gregorian
	tai_utc_difference	[Value of TAI-UTC at time of first record]
	leap_second	YYYY-MM-DDThh:mm:ssZ
	units	seconds since 2000-01-01 00:00:00.000
	comment	Time of measurement in seconds in the UTC time scale since 1 Jan 2000 00:00:00 UTC. [tai_utc_difference] is the difference between TAI and UTC reference time (seconds) for the first measurement of the data set. If a leap second occurs within the data set, the attribute leap_second is set to the UTC time at which the leap second occurs.
double time_tai(num_tvps)		
	_FillValue	9.969209968386869e+36
	long_name	time in TAI
	standard_name	time
	calendar	gregorian
	units	seconds since 2000-01-01 00:00:00.000
	comment	Time of measurement in seconds in the TAI time scale since 1 Jan 2000 00:00:00 TAI. This time scale contains no leap seconds. The difference (in seconds) with time in UTC is given by the attribute [time:tai_utc_difference].
double latitude(num_tvps)		
	_FillValue	9.969209968386869e+36
	long_name	latitude (positive N, negative S) of the spacecraft
	standard_name	latitude
	units	degrees_north
	valid_min	-80.0
	valid_max	80.0
	comment	Geodetic latitude of the KMSF origin with respect to the reference ellipsoid.
double longitude(num_tvps)		
	_FillValue	9.969209968386869e+36
	long_name	longitude (degrees East) of the spacecraft
	standard_name	longitude
	units	degrees_east
	valid_min	-180.0
	valid_max	180.0
	comment	Longitude of the KMSF origin, with positive values indicating longitudes east of the Greenwich meridian.
double altitude(num_tvps)		
	_FillValue	9.969209968386869e+36
	long_name	altitude of the spacecraft

© 2025 California Institute of Technology. Government sponsorship acknowledged.

	units	m
	valid_min	0.0
	valid_max	1000000.0
	coordinates	longitude latitude
	comment	Altitude above the reference ellipsoid of the KMSF origin.
double roll(num_tvps)		
	_FillValue	9.969209968386869e+36
	long_name	roll of the spacecraft
	units	degrees
	valid_min	-180
	valid_max	180
	coordinates	longitude latitude
	comment	KMSF attitude roll angle; positive values move the +y antenna down.
double pitch(num_tvps)		
	_FillValue	9.969209968386869e+36
	long_name	pitch of the spacecraft
	units	degrees
	valid_min	-180
	valid_max	180
	coordinates	longitude latitude
	comment	KMSF attitude pitch angle; positive values move the KMSF +x axis up.
double yaw(num_tvps)		
	_FillValue	9.969209968386869e+36
	long_name	yaw of the spacecraft
	units	degrees
	valid_min	-180
	valid_max	180
	coordinates	longitude latitude
	comment	KMSF attitude yaw angle relative to the nadir track. The yaw angle is a right-handed rotation about the nadir (downward) direction. A yaw value of 0 deg indicates that the KMSF +x axis is aligned with the horizontal component of the Earth-relative velocity vector. A yaw value of 180 deg indicates that the spacecraft is in a yaw-flipped state, with the KMSF -x axis aligned with the horizontal component of the Earth-relative velocity vector.
double velocity_heading(num_tvps)		
	_FillValue	9.969209968386869e+36
	long_name	heading of the spacecraft Earth-relative velocity vector
	units	degrees
	valid_min	0
	valid_max	360
	coordinates	longitude latitude
	comment	Angle with respect to true north of the horizontal component of the spacecraft Earth-relative velocity vector. A value of 90 deg indicates that the spacecraft velocity vector pointed due east. Values between 0 and 90 deg indicate that the velocity vector has a northward component, and values between 90 and 180 deg indicate that the velocity vector has a southward component.
double x(num_tvps)		
	_FillValue	9.969209968386869e+36
	long_name	x coordinate of the spacecraft in the ECEF frame
	units	m
	valid_min	-10000000.0
	valid_max	10000000.0
	comment	x coordinate of the KMSF origin in the ECEF frame.

© 2025 California Institute of Technology. Government sponsorship acknowledged.

double y(num_tvps)		
	_FillValue	9.969209968386869e+36
	long_name	y coordinate of the spacecraft in the ECEF frame
	units	m
	valid_min	-10000000.0
	valid_max	10000000.0
	comment	y coordinate of the KMSF origin in the ECEF frame.
double z(num_tvps)		
	_FillValue	9.969209968386869e+36
	long_name	z coordinate of the spacecraft in the ECEF frame
	units	m
	valid_min	-10000000.0
	valid_max	10000000.0
	comment	z coordinate of the KMSF origin in the ECEF frame.
double vx(num_tvps)		
	_FillValue	9.969209968386869e+36
	long_name	x component of the spacecraft velocity in the ECEF frame
	units	m/s
	valid_min	-10000.0
	valid_max	10000.0
	coordinates	longitude latitude
	comment	KMSF velocity component in x direction in the ECEF frame.
double vy(num_tvps)		
	_FillValue	9.969209968386869e+36
	long_name	y component of the spacecraft velocity in the ECEF frame
	units	m/s
	valid_min	-10000.0
	valid_max	10000.0
	coordinates	longitude latitude
	comment	KMSF velocity component in y direction in the ECEF frame.
double vz(num_tvps)		
	_FillValue	9.969209968386869e+36
	long_name	z component of the spacecraft velocity in the ECEF frame
	units	m/s
	valid_min	-10000.0
	valid_max	10000.0
	coordinates	longitude latitude
	comment	KMSF velocity component in z direction in the ECEF frame.
double plus_y_antenna_x(num_tvps)		
	_FillValue	9.969209968386869e+36
	long_name	x coordinate of the plus_y antenna phase center in the ECEF frame
	units	m
	valid_min	-10000000.0
	valid_max	10000000.0
	comment	x coordinate of the plus_y antenna phase center in the ECEF frame.
double plus_y_antenna_y(num_tvps)		
	_FillValue	9.969209968386869e+36
	long_name	y coordinate of the plus_y antenna phase center in the ECEF frame
	units	m
	valid_min	-10000000.0
	valid_max	10000000.0
	comment	y coordinate of the plus_y antenna phase center in the ECEF frame.
double plus_y_antenna_z(num_tvps)		

© 2025 California Institute of Technology. Government sponsorship acknowledged.

	_FillValue	9.969209968386869e+36
	long_name	z coordinate of the plus_y antenna phase center in the ECEF frame
	units	m
	valid_min	-10000000.0
	valid_max	10000000.0
	comment	z coordinate of the plus_y antenna phase center in the ECEF frame.
double minus_y_antenna_x(num_tvps)		
	_FillValue	9.969209968386869e+36
	long_name	x coordinate of the minus_y antenna phase center in the ECEF frame
	units	m
	valid_min	-10000000.0
	valid_max	10000000.0
	comment	x coordinate of the minus_y antenna phase center in the ECEF frame.
double minus_y_antenna_y(num_tvps)		
	_FillValue	9.969209968386869e+36
	long_name	y coordinate of the minus_y antenna phase center in the ECEF frame
	units	m
	valid_min	-10000000.0
	valid_max	10000000.0
	comment	y coordinate of the minus_y antenna phase center in the ECEF frame.
double minus_y_antenna_z(num_tvps)		
	_FillValue	9.969209968386869e+36
	long_name	z coordinate of the minus_y antenna phase center in the ECEF frame
	units	m
	valid_min	-10000000.0
	valid_max	10000000.0
	comment	z coordinate of the minus_y antenna phase center in the ECEF frame.
int record_counter(num_tvps)		
	_FillValue	2147483647
	long_name	record counter
	units	1
	valid_min	1
	valid_max	999999999
	coordinates	longitude latitude
	comment	Index of the TVP record used to align data samples across granules.
unsigned byte sc_event_flag(num_tvps)		
	_FillValue	255
	long_name	spacecraft event flag
	standard_name	status_flag
	flag_meanings	yaw_flip_maneuver gyro_calibration_maneuver orbit_control_maneuver solar_array_rotation eclipse_entry eclipse_exit karin_bad_due_to_eclipse_event karin_bad_due_to_non_eclipse_event
	flag_masks	1 2 4 8 16 32 64 128
	valid_min	0
	valid_max	255
	coordinates	longitude latitude
	comment	Flag indicating spacecraft events that may affect the characteristics of the KaRIn data. The spacecraft is in a nominal state when all bits equal 0. The KaRIn measurement may be affected by a spacecraft event when any of bits 0 to 5 are equal to 1. The KaRIn measurement is likely bad when bits 6 or 7 are equal to 1.
unsigned byte tvp_qual(num_tvps)		
	_FillValue	255
	long_name	TVP quality flag

© 2025 California Institute of Technology. Government sponsorship acknowledged.

	standard_name	status_flag
	flag_meanings	good orbit_estimated_during_a_maneuver orbit_interpolated_over_data_gap orbit_extrapolated_for_a_duration_less_than_1_day orbit_extrapolated_for_a_duration_between_1_to_2_days orbit_extrapolated_for_a_duration_greater_than_2_days attitude_suspect attitude_suspect_and_orbit_estimated_during_a_maneuver attitude_suspect_and_orbit_interpolated_over_data_gap attitude_suspect_and_orbit_extrapolated_for_a_duration_less_than_1_day attitude_suspect_and_orbit_extrapolated_for_a_duration_between_1_to_2_days attitude_suspect_and_orbit_extrapolated_for_a_duration_greater_than_2_days attitude_bad attitude_bad_and_orbit_estimated_during_a_maneuver attitude_bad_and_orbit_interpolated_over_data_gap attitude_bad_and_orbit_extrapolated_for_a_duration_less_than_1_day attitude_bad_and_orbit_extrapolated_for_a_duration_between_1_to_2_days attitude_bad_and_orbit_extrapolated_for_a_duration_greater_than_2_days
	flag_values	0 4 5 6 7 8 10 14 15 16 17 18 20 24 25 26 27 28
	valid_min	0
	valid_max	28
	coordinates	longitude latitude
	comment	Flag indicating the quality of the reconstructed attitude and orbit ephemeris. A value of 0 indicates the reconstructed attitude and orbit ephemeris are both good. Non-zero values less than 20 indicate suspect data. Values greater than or equal to 20 indicate bad data.

Table 13. Variables of the noise group of the L2_HR_PIXC product.

Group noise Variables		
float noise_plus_y(num_lines)		
	_FillValue	9.96921e+36
	long_name	Noise estimate for the plus_y channel
	units	1
	valid_min	0.0
	valid_max	1e+20
	comment	Noise power for the plus_y channel expressed in linear units (arbitrary units that give noise-equivalent sigma0 when normalized by the X factor).
float noise_minus_y(num_lines)		
	_FillValue	9.96921e+36
	long_name	Noise estimate for the minus_y channel
	units	1
	valid_min	0.0
	valid_max	1e+20
	comment	Noise power for the minus_y channel expressed in linear units (arbitrary units that give noise-equivalent sigma0 when normalized by the X factor).

© 2025 California Institute of Technology. Government sponsorship acknowledged.

6 References

[1] JPL D-105504, "SWOT Algorithm Theoretical Basis Document: Level 2 KaRIn High Rate Pixel Cloud (L2_HR_PIXC) Science Algorithm Software," Jet Propulsion Laboratory Internal Document, 2023.

[2] JPL D-61923, Revision B, "SWOT Science Requirements Document," Jet Propulsion Laboratory Internal Document, 2018.

[3] SWOT-TN-CDM-0677-CNES, Revision C, "SWOT Product Description Document: Level 2 KaRIn High Rate Pixel Cloud Vector Product (L2_HR_PIXCVec)," Centre National d'Etudes Spatiales, 2025.

[4] JPL D-102104, "SWOT Science Data Product Granule Boundary and Sampling Definition," Jet Propulsion Laboratory Internal Document, 2022.

[5] JPL D-56410, Revision C, "SWOT Product Description Document: Level 1B KaRIn High Rate Single Look Complex (L1B_HR_SLC) Data Product," Jet Propulsion Laboratory Internal Document, 2025.

[6] N. K. Pavlis, S. A. Holmes, S. C. Kenyon and J. K. Factor, "The development and evaluation of the Earth Gravitational Model 2008 (EGM2008)," *J. Geophys. Res.: Solid Earth,* vol. 117, pp. 1978-2012, 2012, https://doi.org/10.1029/2011JB008916.

[7] D. E. Cartwright and R. J. Taylor, "New computations of the tide-generating potential," *Geophys. J. R. Astr. Soc.,* vol. 23, pp. 45-74, 1971.

[8] D. E. Cartwright and A. C. Edden, "Corrected tables of tidal harmonics," *Geophys. J. R. Astr. Soc.,* vol. 33, pp. 253-264, 1973.

[9] AVISO, "FES 2022 (Finite Element Solution) - Global Tide," 2024. [Online]. Available: https://doi.org/10.24400/527896/A01-2024.004.

[10] R. D. Ray, "Precise comparisons of bottom-pressure and altimetric ocean tides," *J. Geophys. Res: Oceans,* vol. 118, pp. 4570-4584, 2013.

[11] J. M. Wahr, "Deformation induced by polar motion," *J. Geophys. Res.,* vol. 90(B11), pp. 9363-9368, 1985, https://doi.org/10.1029/JB090iB11p09363.

[12] S. Desai, J. Wahr and B. Beckley, "Revisiting the pole tide for and from satellite altimetry," *J. Geod.,* vol. 89, pp. 1233-1243, 2015, https://doi.org/10.1007/s00190-015-0848-7.

[13] J. C. Ries and S. D. Desai, "Conventional model update for rotational deformation," in *Fall AGU Meeting*, New Orleans, LA, 2017, http://dx.doi.org/10.26153/tsw/2659.

[14] S. Bontemps and e. al., "Global Land Cover Product (2005-06)," European Space Agency, 2005. [Online]. Available: http://due.esrin.esa.int/page_globcover.php.

© 2025 California Institute of Technology. Government sponsorship acknowledged.

Appendix A. **Acronyms**

ATBD	Algorithm Theoretical Basis Document
CNES	Centre National d'Études Spatiales
ECEF	Earth-Centered, Earth-Fixed (frame)
ECMWF	European Centre for Medium-Range Weather Forecasts
GIM	Global Ionosphere Maps
H	Horizontally polarized signal
HPA	High Power Amplifier
HR	High Rate
ITRF	International Terrestrial Reference Frame
JPL	Jet Propulsion Laboratory
KaRIn	Ka-band Radar Interferometer (instrument)
KMSF	KaRIn Metering Structure Frame
LR	Low Rate
NASA	National Aeronautics and Space Administration
NESZ	Noise-Equivalent Sigma Zero
NRCS	Normalized Radar Cross Section
OBP	On-Board Processor
PIXC	Pixel Cloud
SAR	Synthetic Aperture Radar
SLC	Single-Look Complex (radar image)
SNR	Signal-to-Noise Ratio
SWOT	Surface Water and Ocean Topography (mission)
TAI	Temps Atomique International / International Atomic Time
TBC	To Be Confirmed
TBD	To Be Determined
TVP	Time Varying Parameters
UTC	Coordinated Universal Time

© 2025 California Institute of Technology. Government sponsorship acknowledged.

V	Vertically polarized signal
X factor	Radiometric normalization and calibration factor (not an acronym)

© 2025 California Institute of Technology. Government sponsorship acknowledged.

Appendix B. Quality Flag Bit Definitions

Quality flags in SWOT products are sometimes represented as bit flags such that the information from multiple individual conditions is captured in a single flag variable. This is accomplished by defining the flag variable as an unsigned integer whose bits in a binary (base-2 number system) representation reflect the states (true or false) of the individual conditions captured by the flag.

For example, a bit-flag variable q might capture information from three independent binary conditions C_3, C_2, and C_1, each of which might be true or false, in its three least significant bits (LSBs). The value of the variable q would then give the states of C_3, C_2, and C_1 per the table below:

Table 14. Bit Flag Example

Value of q	State of C_3	State of C_2	State of C_1
0	False	False	False
1	False	False	True
2	False	True	False
3	False	True	True
4	True	False	False
5	True	False	True
6	True	True	False
7	True	True	True

Equivalently, the value of the bit-flag variable q is defined mathematically as

$$q = \sum_{k=0}^{n-1} 2^k C_k$$

where n is the number of bits and C_k (whose value is either 0 or 1 to represent the false and true states, respectively) is the condition associated with bit k.

The bit meanings of the *interferogram_qual*, *classification_qual*, *geolocation_qual*, *sig0_qual*, and *pixc_line_qual* flags are given in Table 15.

For each row of the table, the decimal and hexadecimal values represent the value of the flag variable if the bit of that row were 1 and all other bits were 0. All of the information in this table is captured by the *flag_masks* and *flag_meanings* attributes of a given bit-flag variable. Where no condition is specified in the table, the bit is unassigned (not used) and should never be 1. It is possible that these bits will become assigned in future versions of the product, however. The color shading of the table gives a rough, qualitative indication of how much a nonzero bit value for each row would be expected to reduce confidence in the measurement, with redder hues indicating greater degradation.

Table 15. Measurement Quality Flag Bit Definitions

© 2025 California Institute of Technology. Government sponsorship acknowledged.

Bit (from LSB)	Decimal	Hex	interferogram_qual	classification_qual	geolocation_qual	sig0_qual	pixc_line_qual
0	1	1		no_coherent_gain	layover_significant	sig0_uncert_suspect	not_in_tile
1	2	2		power_close_to_noise_floor	phase_noise_suspect	sig0_cor_atmos_suspect	
2	4	4		detected_water_but_no_prior_water	phase_unwrapping_suspect	noise_power_suspect	
3	8	8		detected_water_but_bright_land	model_dry_tropo_cor_suspect	xfactor_suspect	
4	16	10		water_false_detection_rate_suspect	model_wet_tropo_cor_suspect		
5	32	20			iono_cor_gim_ka_suspect		
6	64	40			xovercal_suspect		
7	128	80					
8	256	100					
9	512	200					
10	1024	400	suspect_karin_telem	suspect_karin_telem	suspect_karin_telem	suspect_karin_telem	suspect_karin_telem
11	2048	800	rare_power_suspect	coherent_power_suspect		rare_power_suspect	
12	4096	1000	rare_phase_suspect		medium_phase_suspect		
13	8192	2000	tvp_suspect	tvp_suspect	tvp_suspect	tvp_suspect	tvp_suspect
14	16384	4000	sc_event_suspect	sc_event_suspect	sc_event_suspect	sc_event_suspect	sc_event_suspect
15	32768	8000	small_karin_gap	small_karin_gap	small_karin_gap	small_karin_gap	small_karin_gap
16	65536	10000					
17	131072	20000					
18	262144	40000	in_air_pixel_degraded	in_air_pixel_degraded		in_air_pixel_degraded	
19	524288	80000	specular_ringing_degraded	specular_ringing_degraded	specular_ringing_degraded	specular_ringing_degraded	
20	1048576	100000			model_dry_tropo_cor_missing	sig0_cor_atmos_missing	
21	2097152	200000			model_wet_tropo_cor_missing		
22	4194304	400000			iono_cor_gim_ka_missing		
23	8388608	800000			xovercal_missing		
24	16777216	1000000			geolocation_is_from_refloc		
25	33554432	2000000				noise_power_bad	
26	67108864	4000000				xfactor_bad	
27	134217728	8000000	rare_power_bad	coherent_power_bad	no_geolocation_bad	rare_power_bad	
28	268435456	10000000	rare_phase_bad		medium_phase_bad		
29	536870912	20000000	tvp_bad	tvp_bad	tvp_bad	tvp_bad	tvp_bad
30	1073741824	40000000	sc_event_bad	sc_event_bad	sc_event_bad	sc_event_bad	sc_event_bad
31	2147483648	80000000	large_karin_gap	large_karin_gap	large_karin_gap	large_karin_gap	large_karin_gap

The meanings of the different conditions specified by Table 15 are described below:

- *suspect_karin_telem*: The KaRIn telemetry indicates an off-nominal state (e.g., DORIS tracking flags are not nominal).
- *rare_power_suspect*: The rare power is based on only one SLC channel because the power from the other SLC channel is bad or fails sanity checks.
- *rare_phase_suspect*: The variation in phase between the complex SLC samples that are multilooked to obtain the rare interferogram sample is larger than expected.
- *tvp_suspect*: At least some of the ephemeris or attitude information used for processing is marked suspect.
- *sc_event_suspect*: A spacecraft event such as a maneuver, eclipse transition, etc. may affect the interferogram quality.
- *small_karin_gap*: There is a small gap in the raw KaRIn HR data; a measurement is still computed, but it may have lower quality.
- *in_air_pixel_degraded*: The pixel/range-bin does not intersect the Earth's surface for the corresponding range (hence it is in the air).
- *specular_ringing_degraded*: The interferogram quality is degraded due to range point-target-response side-lobe ringing from a bright target near nadir.
- *rare_power_bad*: Both SLC channels are bad, so no power measurement is available.
- *rare_phase_bad*: At least one SLC channel is bad, so the interferometric phase is not meaningful.
- *tvp_bad*: At least some of the ephemeris or attitude information needed for processing is marked bad.

© 2025 California Institute of Technology. Government sponsorship acknowledged.

- *sc_event_bad*: A spacecraft event such as a maneuver, eclipse transition, etc. likely makes the interferogram quality poor.
- *large_karin_gap*: There is a large gap in the raw KaRIn HR data, or there is no KaRIn HR data at all; a measurement is not computed.
- *no_coherent_gain*: The coherent gain from the coherent power computation is less than 1.
- *power_close_to_noise_floor*: The coherent power is near the estimated noise (low SNR).
- *detected_water_but_no_prior_water*: Water was detected but the prior water probability is low.
- *detected_water_but_bright_land*: Water was detected, but the prior bright-land flag was nonzero.
- *water_false_detection_rate_suspect*: Water was detected, but both the estimated false detection rate is high and the prior water probability is low.
- *coherent_power_suspect*: At least one rare power value used to compute the coherent power is marked suspect, or the coherent gain is less than 1.
- *coherent_power_bad*: Both rare power values used to compute the coherent power are marked bad, or the coherent power fails sanity checks.
- *layover_significant*: The estimated impact due to layover exceeds a threshold.
- *phase_noise_suspect*: Water was detected, and the estimated phase noise standard deviation (computed from the coherence) implies a large height variation.
- *phase_unwrapping_suspect*: The quality of the phase unwrapping solution is questionable based on quality checks related to the ambiguity assignment.
- *model_dry_tropo_cor_suspect*: The model-based correction for dry tropospheric delay is suspect.
- *model_wet_tropo_cor_suspect*: The model-based correction for wet tropospheric delay is suspect.
- *iono_cor_gim_ka_suspect*: The model-based correction for ionospheric delay is suspect.
- *xovercal_suspect*: The crossover-calibration input is flagged as suspect.
- *medium_phase_suspect*: Rare interferogram pixels that are marked suspect are used to compute the medium phase and make it suspect.
- *model_dry_tropo_cor_missing*: The dry-tropospheric delay correction cannot be computed or is not sensical, so no correction is applied.
- *model_wet_tropo_cor_missing*: The wet-tropospheric delay correction cannot be computed or is not sensical, so no correction is applied.
- *iono_cor_gim_ka_missing*: The ionospheric delay correction cannot be computed or

© 2025 California Institute of Technology. Government sponsorship acknowledged.

is not sensical, so no correction is applied.

- *xovercal_missing*: The crossover-calibration correction cannot be computed or is not sensical, so no correction is applied.
- *geolocation_is_from_refloc*: The computed geolocation is not sensical or much farther from the reference location than expected, so the geolocation reported in the product is based on the reference location rather than the measured geolocation.
- *no_geolocation_bad*: The geolocation in the product is not meaningful and the reference location is bad.
- *medium_phase_bad*: The medium phase is not meaningful.
- *sig0_uncert_suspect*: The estimated uncertainty of the sigma0 measurement exceeds a threshold.
- *sig0_cor_atmos_suspect*: The model-based atmospheric attenuation correction is suspect.
- *noise_power_suspect*: The estimate of noise power comes from only one SLC channel because the estimate of the noise power from the other channel is bad or not sensical.
- *xfactor_suspect*: The X factor comes from only one SLC channel because the X factor for the other channel is bad or not sensical.
- *sig0_cor_atmos_missing*: The model-based atmospheric attenuation correction is missing or bad.
- *noise_power_bad*: The estimate of noise power is bad or not sensical for both SLC channels.
- *xfactor_bad*: The X factor is bad or not sensical for both SLC channels.
- *not_in_tile*: The line is outside the tile granule.

© 2025 California Institute of Technology. Government sponsorship acknowledged.